UiT
THE ARCTIC UNIVERSITY OF NORWAY

Faculty of Health Sciences

Predicting rupture of intracranial aneurysms

Morphological and hemodynamic parameters

—

Torbjørn Øygard Skodvin

A dissertation for the degree of Philosophiae Doctor – April 2018

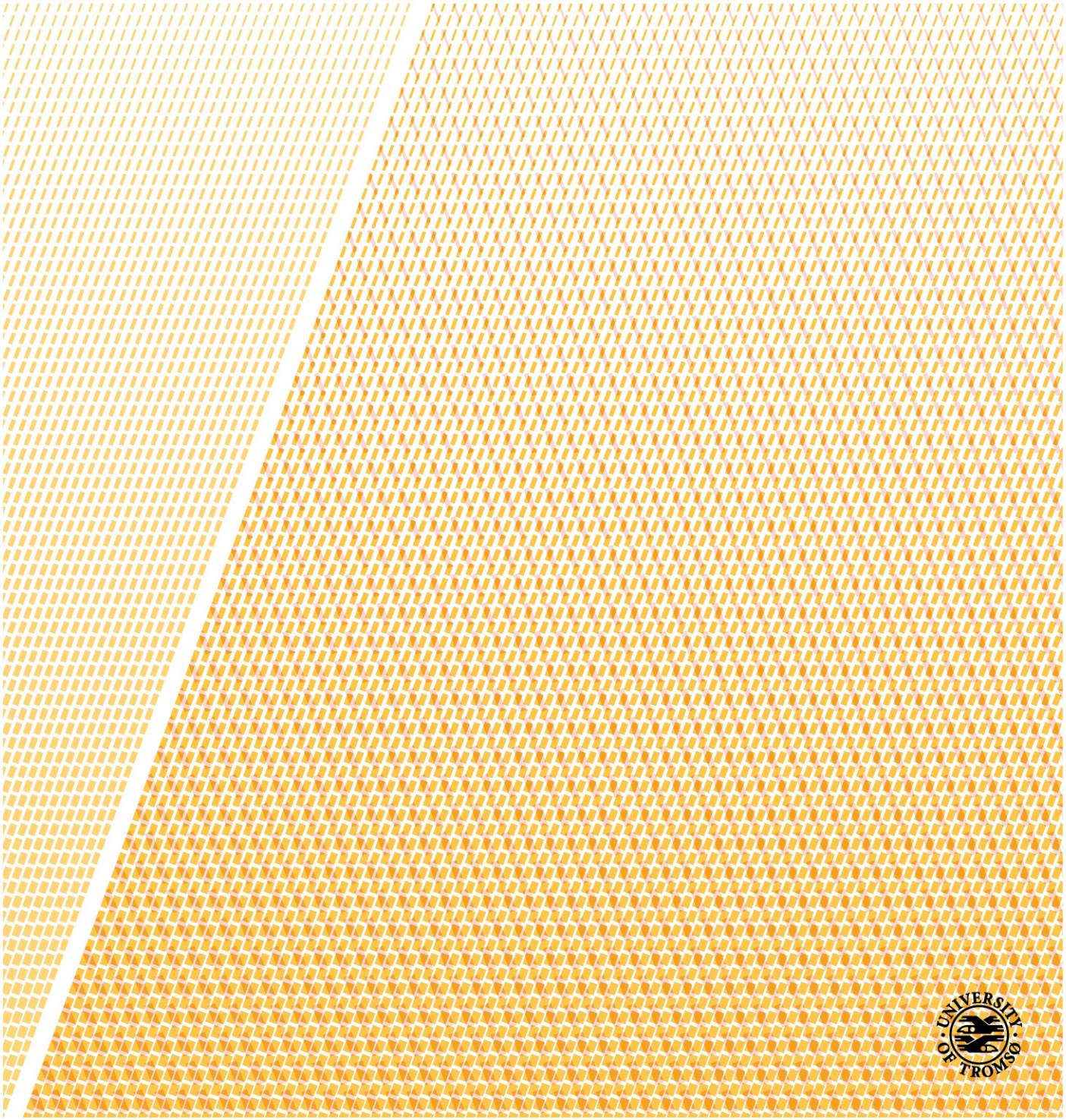

“Once you stop learning,
you start dying.”

Albert Einstein (1879 – 1955)

Contents

1 Acknowledgments

My sincere thanks go to everyone involved in this thesis.

Jørgen Gjernes Isaksen, supervisor, believed in me a long time before I knew what research was. I am inspired by his sharp knowledge, humble and curious attitude, and patient-centered care. He has influenced both my medical career and personal character.

Roar Kloster and Tore Solberg, cosupervisors, have lent me their bright minds and constructive comments, and greatly improved the thesis. Ellisiv B. Mathiesen, head of the Brain and Circulation Research Group, has cared for both me and my family, and guided me with her extensive experience. The members of the research group have held presentations, discussions, and different perspectives that I have greatly enjoyed and learnt from.

Coauthors Liv-Hege Johnsen, Øyvind Evju, Angelika Sorteberg, Øivind Gjertsen and Christian A. Helland, your contributions have substantially improved the included papers. Thanks to Ole Solheim and the radiological departments at the four hospitals where my data was collected for invaluable help and preparations. Tom Wilsgaard, thank you for statistical help. Haakon Lindekleiv and Tor Ingebrigtsen, thank you for your valuable time, ideas, and strategical discussions.

My parents, Kristin and Kjell Gunnar, and brothers and sisters Øyvind, Sigrun, Helga and Tobias, thank you for your neverending support and curiosity. Thanks to my closest friends for engaging conversations and fun distractions.

Linn Kristin, my greatest love, sharpest critic and dearest support, and our beautiful daughters, Signa Naomi and Agnes Annie — thank you for being the ones you are. You are the stars of my show.

2 Abstract

English abstract

BACKGROUND Because of extended use of cerebral imaging, unruptured intracranial aneurysms are increasingly discovered as incidental findings. Management of unruptured aneurysms is controversial because patients and clinicians must weigh the risks of prophylactic endovascular or surgical treatment against the uncertain risk of rupture. We aimed to investigate the use of hemodynamic and morphological parameters of intracranial aneurysms to predict rupture risk.

METHODS We performed a nationwide retrospective data collection from electronic health records. By means of diagnosis and procedure codes, we identified patients with known but untreated saccular intracranial aneurysms that later were hospitalized with subarachnoid hemorrhage. We collected cerebral imaging at the time of diagnosis, and before and right after rupture. We investigated morphological parameters at all these points of time, and hemodynamic parameters at the time of diagnosis. In a case series, we compared morphological parameters before and after rupture. In matched case-control studies, we compared morphological and hemodynamic parameters at the time of diagnosis between aneurysms that later ruptured with aneurysms that remained unruptured.

RESULTS We identified 43 patients with a saccular aneurysm that later ruptured. The aneurysms appeared larger and more irregular after rupture than before rupture. Aneurysms that later ruptured had a straighter inflow angle in relation to the parent artery, compared to aneurysms that remained unruptured. Aneurysms that later ruptured had a larger low shear area than aneurysms that remained unruptured.

CONCLUSION The postrupture morphology of intracranial aneurysms is inadequate as a surrogate for the prerupture morphology in the evaluation of rupture risk. Hemodynamic and morphological parameters at the time of diagnosis of unruptured aneurysms that later rupture can be different from aneurysms that remain unruptured.

Norwegian abstract – norsk sammendrag

Å forutse ruptur av intrakraniale aneurismer

Morfologiske og hemodynamiske parametre

BAKGRUNN Økende bruk av cerebral bildediagnostikk gjør at vi stadig oftere oppdager ikke-rumperte intrakraniale aneurismer som tilfeldig bifunn. Håndteringen av disse er omdiskutert fordi pasienter og klinikere må veie risikoen ved profylaktisk endovaskulær eller kirurgisk behandling opp mot den ukjente risikoen for ruptur. Vi ønsket å undersøke hvordan hemodynamiske og morfologiske parametre ved intrakraniale aneurismer kan brukes til å forutsi risiko for ruptur.

METODE Vi utførte en nasjonal retrospektiv datainnsamling fra pasientjournaler. Ved hjelp av diagnose- og prosedyrekoder identifiserte vi pasienter med kjente men ikke behandlede sakkulære intrakraniale aneurismer som senere ble innlagt i sykehus med subaraknoidalblødning. Vi samlet inn bildediagnostikk på diagnosetidspunkt, og før og etter ruptur. Vi undersøkte morfologiske parametre på alle disse tidspunktene, og hemodynamiske parametre på diagnosetidspunkt. I en kasusserie undersøkte vi morfologiske parametre før og etter ruptur. I kasus-kontrollstudier sammenlignet vi morfologiske og hemodynamiske parametre på diagnosetidspuhnkt, mellom aneurismer som senere rumperte og aneurismer som forble uten ruptur.

RESULTAT Vi identifiserte 43 pasienter med et sakkulært aneurisme som senere rumperte. Aneurismene fremsto større og mer irregulære etter ruptur enn før. Aneurismer med fremtidig ruptur hadde en rettere innstrømsvinkel i forhold til moderarterien enn aneurismer som forble uten ruptur. Aneurismer med fremtidig ruptur hadde større areal med lav skjærspenning enn aneurismer som forble uten ruptur.

KONKLUSJON Postruptur-morfologi av intrakraniale aneurismer er inadekvat som surrogat for preruptur-morfologi i vurdering av rupturrisiko. Hemodynamiske og morfologiske parametre av ikke-rumperte aneurismer med fremtidig ruptur kan være forskjellig på diagnosetidspunkt sammenlignet med aneurismer som forblir uten ruptur.

Kandidat	Torbjørn Øygard Skodvin
Institutt	Institutt for Klinisk Medisin
Hovedveileder	Jørgen Gjernes Isaksen
Biveileder	Roar Kloster
Biveileder	Tore K. Solberg
Finansiering	Helse Nord og UiT Norges Arktiske Universitet

3 Abbreviations

ACoA	anterior communicating artery
aSAH	aneurysmal subarachnoid hemorrhage
CT	computed tomography
CTA	computed tomography angiography
DSA	digital subtraction angiography
ESP	European Standard Population
IA	intracranial aneurysm
ICA	internal carotid artery
ICI	inflow concentration index
IQR	interquartile range
LSA	low shear area
MCA	middle cerebral artery
MMP	matrix metalloprotease
MRA	magnetic resonance angiography
MRI	magnetic resonance imaging
PCoA	posterior communicating artery
PHASES	population, hypertension, age, size of aneurysm, earlier SAH from another aneurysm, site of aneurysm
PLc	pressure loss coefficient
SAH	subarachnoid hemorrhage
SNP	single-nucleotide polymorphism
TNF	tumor necrosis factor
UIATS	unruptured intracranial aneurysm treatment score
WSS	wall shear stress

4 List of papers

I. **Cerebral aneurysm morphology before and after rupture: nationwide case series of 29 aneurysms.**
Skodvin, T. Ø., Johnsen, L. H., Gjertsen, Ø., Isaksen, J. G., Sorteberg, A.
Stroke 2017; *48*(4): 880–886.

II. **Rupture prediction of cerebral aneurysms: a nation-wide matched case-control study of hemodynamics at time of diagnosis.**
Skodvin, T. Ø., Evju, Ø., Helland, C. A., Isaksen, J. G.
Journal of Neurosurgery (e-published ahead of print Nov 3, 2017)

III. **Prerupture intracranial aneurysm morphology in predicting risk of rupture: A matched case-control study.**
Skodvin, T. Ø., Evju, Ø., Sorteberg, A., Isaksen, J. G.
Neurosurgery (e-published ahead of print Feb 26, 2018)

The papers will be referred to by their Roman numerals throughout the thesis.

5 Introduction

Disease that affects the brain necessarily affects a person's identity, meaning and interpretation of life.[76] Intracranial aneurysms (IA) are found in 2-3.5% of the general adult population.[113,170] The prevalence varies with risk factor load, and can be over 20% in some subgroups.

About a quarter of IA will rupture during the patient's lifetime and cause a subarachnoid hemorrhage (SAH).[83] SAH occurs at a relatively low average age, with a case fatality of almost 50%, and half of the survivors suffering permanent disability. Therefore, SAH is a devastating disease for patients, their families, and society.[132,149]

Wider availability and use of cerebral imaging has led to growing numbers of incidentally discovered unruptured IAs.[147] The risk of rupture increases with the size of the aneurysm, but the majority of SAH originate from small aneurysms.[10] The management of unruptured IAs remains controversial, because the risk of complications connected to prophylactic treatment must be weighed against the unknown risk of rupture for an individual aneurysm.[19]

5.1 What this thesis is about

This thesis investigates hemodynamic and morphological predictors for the rupture of an IA, in a population of patients with known and untreated unruptured IA. The thesis comprises one case series and two matched case-control studies.

Improved rupture prediction can guide treatment decisions and ensure that high-risk aneurysms are treated prophylactically, while sparing patients with benign aneurysms from unnecessary treatment that involves considerable risk.

The Introduction chapter considers literature published up to Fall 2017. However, section 5.4 mostly considers literature up to Fall 2013, to reflect the status of research on hemodynamic and morphological rupture predictors when I started my work.

5.2 Subarachnoid hemorrhage

Worldwide, stroke is the second largest cause of death and life years lost, after ischemic heart disease.[43] Subarachnoid hemorrhage (SAH) is a subtype of stroke, caused by bleeding into the subarachnoid space surrounding the brain. SAH is the third most common presentation of stroke

(~5%), after ischemic stroke (~85%) and intracerebral hemorrhage (~10%).[44] However, SAH occurs at younger age and entails higher mortality and morbidity, resulting in a greater loss of productive life.[93] Therefore, the socioeconomic burden from SAH is comparable to that of ischemic stroke and intracerebral hemorrhage.[132]

Ruptured saccular intracranial aneurysms account for 85% of SAHs.[164] This hemorrhage is the subject of this thesis, and will be denoted aneurysmal subarachnoid hemorrhage (aSAH). Other common causes include trauma, rupture of arteriovenous malformations, and arterial dissection.[143]

5.2.1 Epidemiology

5.2.1.1 Incidence

Studies of aSAH incidence must be interpreted with caution. Many original studies have few aSAH events and employ highly variable case-finding methods.

In Norway, European Standard Population (ESP) standardized incidence was 8.7 per 100,000 person-years between 1984 and 2007.[136] This incidence may be underestimated because 20% of aSAH deaths occur immediately and out of hospital,[87] and Norway has the lowest autopsy rate among Nordic countries.[82] Formerly, the neighbouring country Finland has been described as a high-incidence country, but recent registry-based studies probably provides more correct estimates of the nationwide incidence.[85] ESP standardized incidence was 12.3 per 100,000 person-years between 1987 and 2002 in Denmark,[36] and 8.9 per 100,000 person-years between 2010 and 2012 in Finland.[85] Because of long life-expectancy in the Nordic countries, ESP standardized incidences are lower than crude incidences.[82]

Worldwide, the incidence of aSAH is estimated to 9.1 per 100,000 persons per year (95 % Confidence interval [CI], 8.8 to 9.5), according to meta-analysis comprising 51 prospective studies from 21 countries.[31,100] Though the study represents an important effort to map regional variations and time trends of aSAH incidence, the estimate is uncertain because many of the included studies had less than 15 SAH patients and showed large variations.

The incidence of aSAH is declining along with the decrease in cardiovascular risk factors.[85] In the Norwegian Tromsø Study cohort, annual crude incidence per 100,000 person-years declined from 11.1 to 8.9 between 1999 and 2007.[95] Finland has had a similar decline, with the 3-year average of the ESP incidence reduced from 11.7 to 8.9 between 1998 and 2012.[85]

The incidence is highest among women and for the age group between 50 and 69 years.[136] The female/male incidence ratio peaks at 2.9 between 50 and 59 years.[136]

5.2.1.2 Risk factors

aSAH incidence is closely related to IA prevalence (see section 5.3). That is, the factors increasing aSAH risk are mostly factors that increase risk of carrying an IA.

The most important risk factors for aSAH are female sex, smoking and high blood pressure. Each of these doubles the risk of carrying an aneurysm,[78,170] but the risk increases exceptionally when several factors are combined.[86,98] The three risk factors account for most of the variation in aSAH incidence, as illustrated in a Finnish study: the incidence of aSAH among female smokers with high systolic blood pressure (≥159 mmHg) was 20-fold higher than among male never-smokers with low systolic blood pressure (≤122 mmHg).[86]

The female preponderance starts around age 55, likely because the lower estrogen levels during and after menopause leave arteries more vulnerable for aneurysm formation.[22] Also, female cerebrovascular anatomy may contribute to more frequent aneurysms,[96] and women with aneurysms may be more vulnerable for risk factors such as smoking.[97] Smoking causes arterial wall inflammation and an increased hemodynamic load, and hypertension is closely related to endothelial dysfunction, contributing to the abnormal inflammatory response.[22]

Excess alcohol consumption increases aSAH risk,[42] whereas overweight (BMI 25-29.9) may be protective.[135] The relations between aSAH and oral contraceptives, hormonal replacement therapy, serum lipids and physical exercise are uncertain.[42,135] Many studies are small and retrospective, making risk factor assessments difficult and prone to bias.[82]

Genes and environment

Family history of SAH may increase risk threefold,[170] and screening for IA is recommended for individuals with two or more first-degree relatives with SAH.[13,147,155] Non-white ethnicity may double aSAH risk, though estimates are uncertain.[42] (Finnish and Japanese ethnicity has formerly been assumed to increase aSAH risk, but this might merely reflect the scarcity of robust studies.[82,85])

The increased risk is most often attributed to a shared family and ethnic environment rather than genetic factors.[22,84] The largest twin study to date, with more than 6 million person-years of follow-up time, concluded that SAH appears to be mainly of nongenetic origin.[84] However, environmental risk factors can influence genetic expression,[49] which makes identification of genes associated with aneurysms difficult.[22] A meta-analysis of 61 studies, including almost 33,000 aneurysm patients,

identified three single-nucleotide polymorphisms (SNPs) that were associated with presence of sporadic aneurysms. The strongest association showed an odds ratio of 1.29, and the SNPs were mainly related to vascular endothelial maintenance.[2]

Though aSAH is mainly of nongenetic origin, rare hereditary diseases increase IA and aSAH risk substantially. Autosomal dominant polycystic kidney disease is the hereditary disease most commonly associated with SAH. The disease affects 1 out of every 1,000 individuals,[116] and 10-23 % of these may harbor aneurysms.[24,170] The disease is caused by mutation in genes that are also expressed in vascular smooth muscle and the endothelium.[134] Other hereditary diseases associated with IAs and SAH are Ehlers-Danlos syndrome type IV (caused by mutation of collagen type III), fibromuscular dysplasia, and possibly Marfan syndrome (mutation of fibrillin-1 gene).[23]

Multiple aneurysms are found in 20-30% of aneurysm patients. Most likely, both individual anatomical variants, genetic factors and environmental risk factors act in concert to give rise to multiple aneurysms in the same patient.[22]

Trigger factors

A subset of risk factors are those that provoke immediate rupture—trigger factors. Trigger factors are related to a sudden increase in the systemic blood pressure, and include caffeine consumption, vigorous physical exercise, anger, startling, straining for defecation, sexual intercourse and nose blowing.[169] Still, most aSAH occur during normal and unstrained activities of daily living.[106]

5.2.2 Pathogenesis and clinical presentation

Immediately after the rupture of IA, the arterial pressure pushes blood into the subarachnoid space. A small bleeding might self-terminate, whereas a larger bleeding continues until the intracranial pressure equalizes across the rupture site and stops the bleeding with thrombus formation.[93]

At the microscopic level, the acute phase is dominated by the deposition of red blood cells in the subarachnoid space. When the red blood cells degrade, they activate inflammatory processes allowing a multitude of inflammatory cells to enter the subarachnoid space.[104] In the subacute phase, macrophages and neutrophils in the subarachnoid space release inflammatory agents inducing vasoconstriction, meningitis and cerebritis.[104]

The hallmark presenting symptom of subarachnoid hemorrhage is “the worst headache of my life”, known as thunderclap headache reaching maximum intensity within seconds.[93,164] Typically within two weeks before the hemorrhage,[101] 10 to 43 % of patients experience a warning leak or sentinel headache—a hyperacute pain unlike headaches the patient might have experienced before, without

evidence of bleeding.[125] Subarachnoid hemorrhage is commonly associated with nausea, vomiting, photophobia, neck stiffness, focal neurologic deficits and a brief loss of consciousness. More severely affected patients present with persisting consciousness disturbance, ranging from mild lethargy to profound coma and death.[93]

Following aneurysm rupture, a number of complications add to the severity and complexity of SAH:

- Early rebleeding within the first days occurs in about 15 % of untreated patients, with over 50 % mortality;[120]
- Hydrocephalus occurs in 15 to 85 % of patients because of extravasation of blood blocking normal cerebrospinal fluid circulation. Whereas some cases are not clinically significant, 9 to 50 % of patients will have chronic shunt-dependent hydrocephalus;[29]
- Intraparenchymal hematomas may occur close to the rupture site and give focal neurological deficits, mass effect, and raised intracranial pressure;[149,164]
- Vasospasm is angiographically visible in 70 % of patients, typically starting 3-4 days after SAH, peaking at 7 to 10 days, and resolving within 14 to 21 days. Delayed Cerebral Ischemia is a clinical syndrome of focal neurologic deficits that occurs in a third of patients. The ischemia can progress to cerebral infarction, which for 50% of patients results in severe disability or death.[133] Delayed Cerebral Ischemia has traditionally been ascribed to vasospasm, but the exact pathogenesis remains incompletely understood—not all patients with vasospasm have neurological deterioration, and neither do all patients with clinical features of Delayed Cerebral Ischemia have vasospasm.[166] Thus, other factors must also be involved in the pathogenesis, such as a widespread cerebral inflammation.[104,166]
- Systemic complications arise in the vast majority of patients, and can be severe in 40% of cases. The most common complications include pulmonary edema, cardiac arrhythmias and electrolyte disturbances.[149] The pathophysiology can be complex and sometimes obscure.[29,104]

5.2.2.1 Diagnostic workup

The first essential step for diagnosing aSAH diagnosis is cerebral Computed Tomography (CT) scan without contrast enhancement. Typically, the scan shows blood distributed in the subarachnoid space, including basal cisterns, sometimes accompanied by hydrocephalus and/or intracerebral or intraventricular hemorrhage (Figure 1).[93,147] Within the first three days, the sensitivity of a CT scan is near 100 %,[93] but later the sensitivity of Magnetic Resonance Imaging (MRI) is superior to CT.[147]

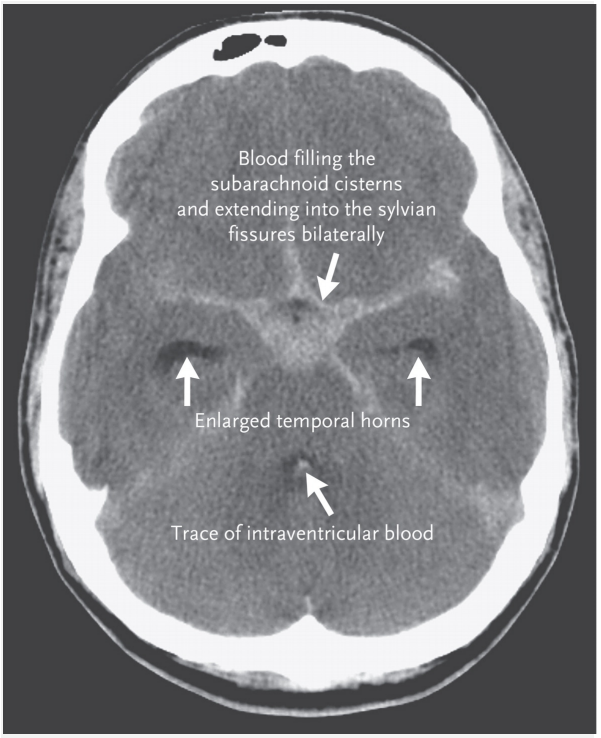

Figure 1. CT scan of the head showing evidence of subarachnoid hemorrhage. A thick blood clot (≥1 mm thick) can be seen in the cerebrospinal fluid–filled cisterns around the circle of Willis. The greater amount of blood in the left basal cisterns than in the right points to a likely location of the aneurysm on the left side of the cerebral circulation. The enlarged temporal horns are evidence of hydrocephalus; in most patients (and especially in younger patients) the temporal horns should not be visible. Reproduced with permission from Lawton MT, Vats GE: Subarachnoid Hemorrhage. ***N Engl J Med 377****:257–266, 2017. Copyright Massachusetts Medical Society.*

In case of a clinically suspected SAH with negative or uncertain CT or MRI findings, lumbar puncture may be performed to detect a minor subarachnoid hemorrhage, i.e. red blood cell degradation products including bilirubin and oxyhemoglobin. To allow time for the degradation, lumbar puncture is recommended 6-12 hours at the earliest after SAH. Waterclear, normal cerebrospinal fluid (CSF) excludes SAH within the last 2-3 weeks, whereas the detection of xanthocromia of the CSF increases likelihood of SAH. A bloody CSF may be caused by a traumatic tap.[147]

Computed tomography angiography (CTA) and magnetic resonance angiography (MRA) have sensitivity and specificity close to 1 for aneurysms larger than 3 mm.[163] However, the aneurysm neck, which is important when deciding between endovascular or surgical treatment, tends to be overestimated.[55] MRA suffers from signal loss in areas of low or complex flow and may not completely display the entire geometry of an aneurysm.[58] The gold standard for detecting and localizing ruptured aneurysms is digital subtraction angiography (DSA), but this procedure requires arterial puncture and catheterization.[147] All three modalities provide solutions for 3D visualization of the anatomy. A version of DSA, 3D rotational angiography, allows reformatted images to be rotated. In CTA and MRA, 3D-models are software-generated from the original thin-section 2D images.[18]

Figure 2 shows aneurysms before and after treatment using DSA and CTA.

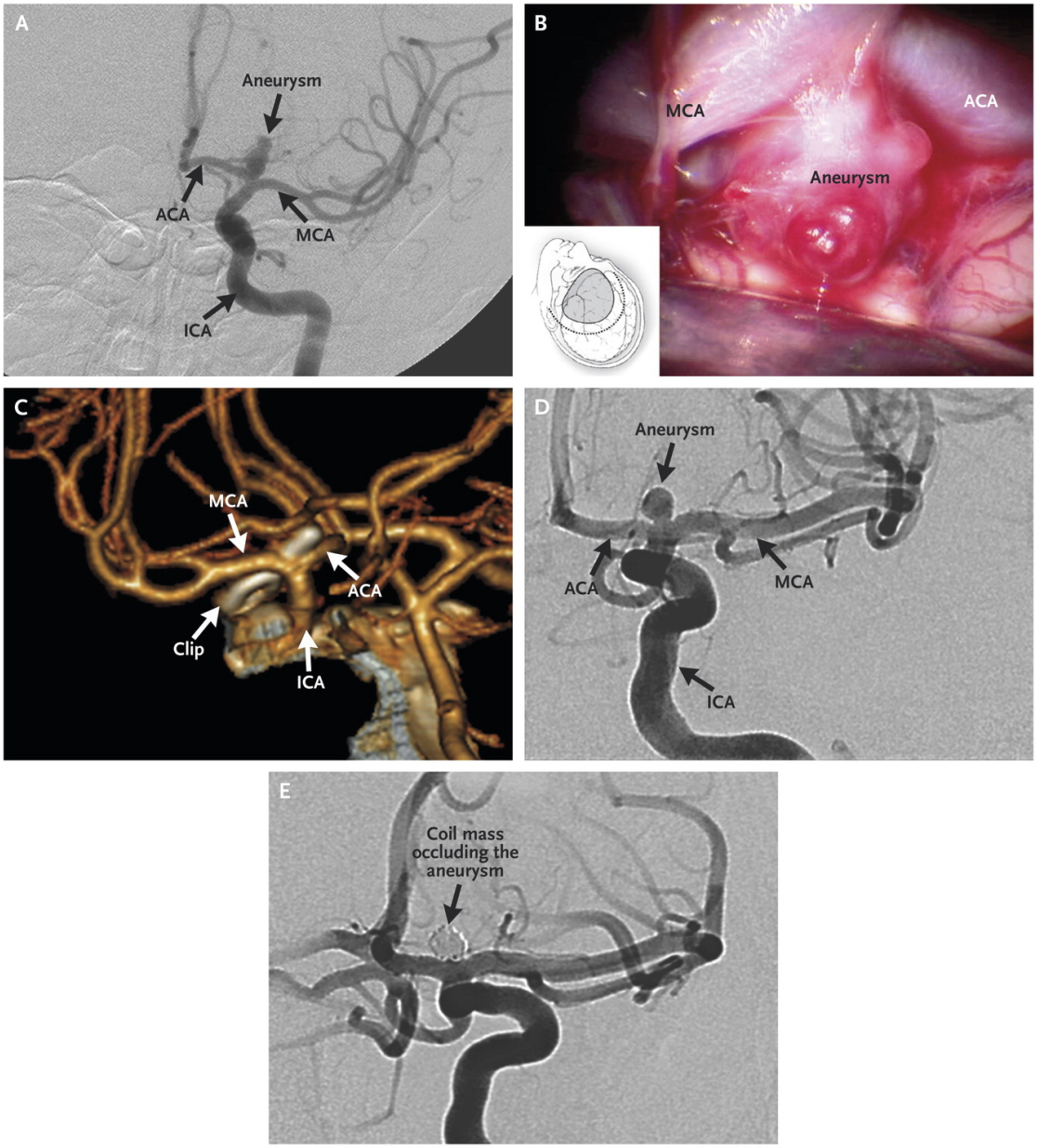

Figure 2. Angiogram showing internal carotid artery (ICA) aneurysms before and after treatment. The aneurysm originates at the point where the ICA bifurcates into the arterial cerebral artery (ACA) and the middle cerebral artery (MCA) (Panel A). At the time of surgery, the aneurysm was exposed and was shown to be multilobulated, very thin-walled, and with friable daughter lobules (Panel B; the inset shows the location of the aneurysm in the patient's brain). CT angiography shows the placement of a surgical clip and complete obliteration of the aneurysm (Panel C). An angiogram obtained in a different patient shows a similarly located ICA aneurysm (Panel D) and the results obtained with endovascular treatment (Panel E). Reproduced with permission from Lawton MT, Vates GE: Subarachnoid Hemorrhage. ***N Engl J Med 377****:257–266, 2017. Copyright Massachusetts Medical Society.*

5.2.2.2 Grading

Several grading systems exist for classifying the severity of SAH. The most frequently used grades are the Hunt & Hess score and the World Federation of Neurosurgical Societies (WFNS) grade for clinical assessment,[93] and the radiological Fisher grade.[47] The grading systems are shown below (Table 1). Both clinical scores classify patients based on increasing severity of encephalopathy. The radiological score evaluates the amount and distribution of SAH on CT scans.[70]

Table 1. Clinical and radiological grading systems for classifying the severity of subarachnoid hemorrhage (year of publication in parentheses).

Hunt & Hess (1968)

I	asymptomatic, or minimal headache and slight nuchal rigidity
II	moderate to severe headache, nuchal rigidity, no neurologic deficit other than cranial nerve palsy
III	drowsiness, confusion, or mid focal deficit
IV	stupor, moderate to severe hemiparesis, possibly early decerebrate rigidity and vegetative disturbances
V	deep coma, decerebrate rigidity, moribund appearance

WFNS (1998)

I	GCS* 15, no motor deficit
II	GCS 13-14, no motor deficit
III	GCS 13-14 + motor deficit
IV	GCS 7-12 +/- motor deficit
V	GCS 3-6 +/- motor deficit

*) Glasgow Coma Scale

Fisher (1980)

I	No blood
II	Diffuse or thin layer of blood less than 1 mm thick (interhemispheric, insular, or ambient cisterns)
III	Localized clots and/or layers of blood greater than 1 mm thick in the vertical plane
IV	Intracerebral or intraventricular clots with diffuse or absent blood in basal cisterns

5.2.3 Treatment

After initial stabilization or resuscitation, the prevention of rerupture is the first treatment goal. Next is prevention and treatment of the complications associated with SAH.

5.2.3.1 Prevention of rerupture

Medical steps to reduce the risk of rerupture include treatment of high blood pressure, and antifibrinolytic therapy to stabilize the initial thrombus at the bleeding site. Also, seizures are treated as they can cause hemodynamic instability triggering aneurysm rerupture.[93]

Definite treatment of the ruptured aneurysm can be achieved by surgical clipping or endovascular aneurysm obliteration (Figure 3), and should be performed as early as feasible in the majority of patients.[29,93] Surgical clipping requires opening of the scull (craniotomy) and microscopy-assisted

mobilizing of brain tissue to expose the aneurysm, and placing a metal clip across the aneurysm neck. The goal is to close the aneurysm sac from the outside, while leaving normal blood flow in the adjacent arteries. Endovascular techniques involve arterial catheterization, usually with access from the femoral artery in the groin. The catheter is navigated to and advanced into the aneurysm sac to deposit metal coils.[93] Thus, the aneurysm is excluded from the circulation from the inside, and the slow or stagnant intraaneurysmal flow induces thrombosis.[60]

Two randomized trials comparing surgical and endovascular methods showed better functional outcomes after one year with endovascular treatment, though open microsurgery had a significantly higher rate of obliteration and greater durability.[110,111,145,146] However, comparing the two methods is difficult, since an aneurysm may be more accessible and treatable by one of them. Indeed, in one of the trials, the International Subarachnoid Trial (ISAT), only 22.4% of patients met the inclusion criteria of an equally coilable or clippable aneurysm, resulting in a highly selected study sample.[111] Development of and experience with both methods have resulted in better obliteration rates for endovascular treatment, and less morbidity for surgical treatment.[145] Current recommendations state that surgical treatment is the preferred option for aneurysms with a wide neck, branching vessels out of the aneurysm sac, middle cerebral artery and pericallosal artery aneurysms (because of accessibility) or patients with intracerebral hematoma that require surgical evacuation.[29,147] Endovascular treatment is particularly recommended for aneurysm with small neck of the basilar artery or elsewhere in the posterior circulation, and elderly patients (>70 years). Because of the complexity of the treatment, treatment decisions should be interdisciplinary.[29,147]

Endovascular techniques have evolved and improved rapidly the last two to three decades. Newer techniques under investigation include stent-assisted coiling, balloon-assisted coiling, flow diverters and disruptors, and new embolic material. The rapid development of new techniques offers hope of increased aneurysm obliteration, and that aneurysms previously considered untreatable may be treatable in the future.[124] However, the techniques have been associated with increased morbidity and mortality. Due to lack of data on complications and long-time effects, these techniques are recommended only when less risky options have been considered.[29]

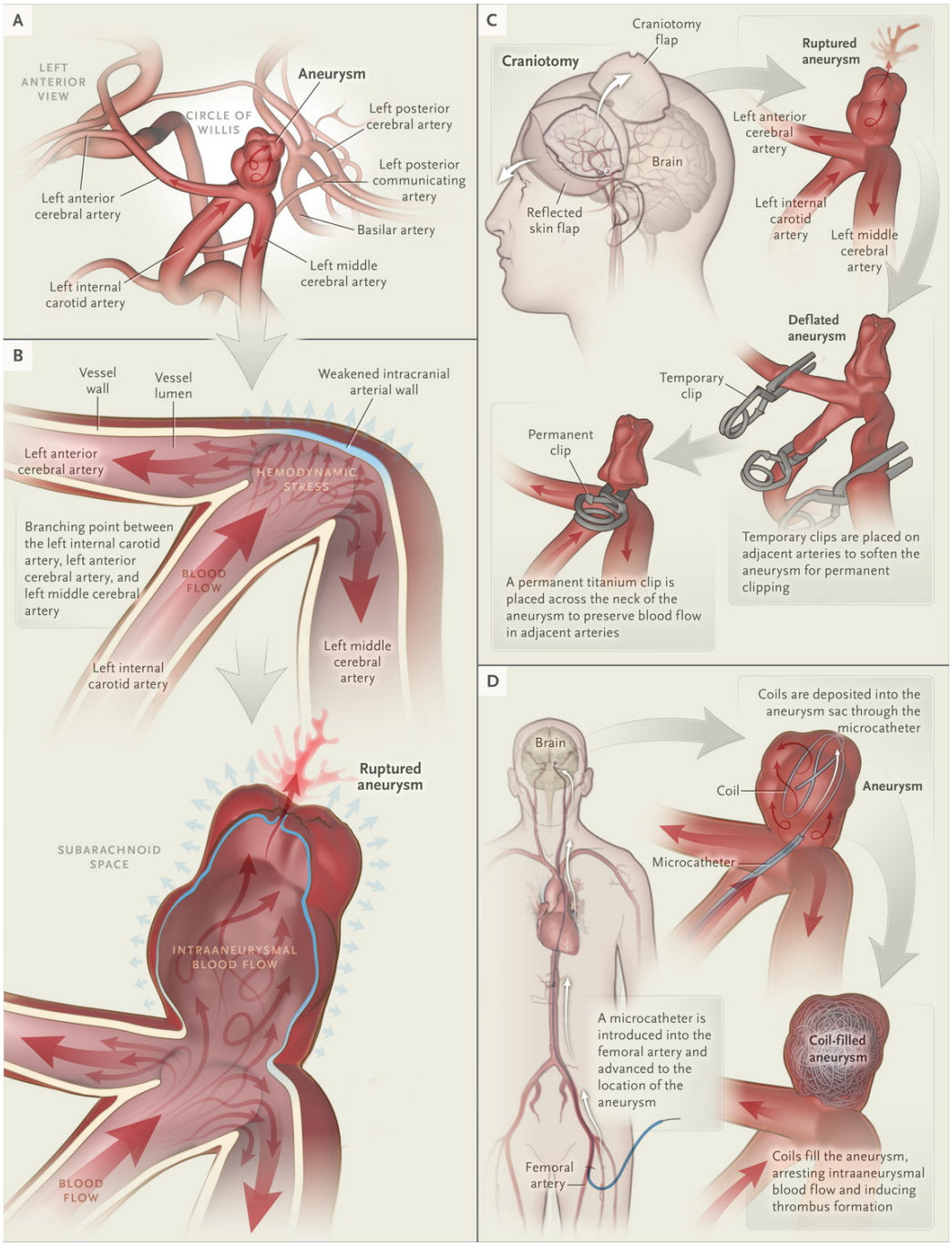

*Figure 3. Repair of aneurysms that have caused subarachnoid hemorrhage. The anatomy of the subarachnoid space and the circle of Willis is shown in Panel A. An aneurysm has formed at a branching point and ruptures (Panel B). Open surgical repair of such an aneurysm (Panel C) involves exposing the aneurysm and the adjacent normal arteries so that the surgeon can apply a titanium clip on the neck of the aneurysm, which effectively excludes it from the arterial circulation. Removal of portions of the skull base provides improved access and operative exposure for the surgeon without the need for substantial brain retraction. Endovascular repair of such an aneurysm (Panel D) involves the navigation of an intraarterial catheter through the circulation under fluoroscopic guidance until the catheter tip is in the lumen of the aneurysm. With the use of the catheter, platinum coils are delivered and packed into the lumen of the aneurysm, which slows or prevents blood flow into the aneurysm and leads to thrombus formation, effectively blocking arterial blood from entering the aneurysm. Reproduced with permission from Lawton MT, Vates GE: Subarachnoid Hemorrhage. **N Engl J Med 377**:257–266, 2017. Copyright Massachusetts Medical Society.*

5.2.3.2 Prevention and treatment of complications

Clinically significant hydrocephalus is alleviated with external ventricular or lumbar drainage, which can be converted to a permanent ventriculoperitoneal shunt to manage chronic hydrocephalus.[93] To prevent delayed cerebral ischemia, the oral calcium antagonist nimodipine is recommended for all patients from presentation to 21 days after SAH.[93] A Cochrane review of randomized trials reported that nimodipine reduced the risk of poor outcomes in aSAH patients by one third.[33] Acute treatment with statins has been suggested to reduce delayed cerebral ischemia, but metaanalyses have neither shown effect on neurological outcomes nor death.[165,180]

Because of the extensive systemic complications associated with aSAH, patients should be treated in neurointensive care units. In general, the treatment aims at keeping the patient normovolemic, normothermic, avoiding hypoglycemia or marked hyperglycemia, and seizure free. Anticoagulation is administered to avoid deep venous thrombosis, when the aneurysm is secured and if the general bleeding risk is acceptable.[93]

5.2.3.3 Outcome: mortality and morbidity

Six months after aSAH, 40% of patients in two Norwegian cohorts had died. The fatality rate was high during the first month before leveling off (Figure 4); case fatality at 1, 3, 7, and 30 days was 14%, 20%, 24% and 36%, respectively.[136] The case fatality rate has decreased slightly over the last decades.[1,117] Internationally, the rate varies substantially—between 25 and 50%[117]—with the highest rates in low- and middle-income countries.[1,44]

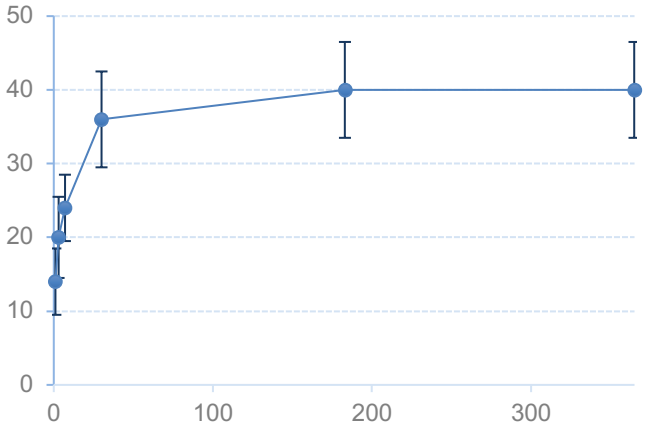

*Figure 4. Percentage of deceased patients in days after aneurysmal subarachnoid hemorrhage. Error bars show 95% confidence intervals. Adapted from Sandvei MS, Mathiesen EB, Vatten LJ, Muller TB, Lindekleiv H, Ingebrigtsen T, et al: Incidence and mortality of aneurysmal subarachnoid hemorrhage in two Norwegian cohorts, 1984-2007. **Neurology 77**:1833–1839, 2011.*

The most important prognostic factor of outcome is the clinical state at presentation, with a lower Glasgow Coma Scale (and higher Hunt & Hess and WFNS scores) corresponding to a worse outcome.[93] Patient age and the amount of extravasated blood on CT scans are next most important.[121,147] Although the Fisher grade is commonly used to predict the risk of cerebral vasospasm, more recent scales use quantitative approaches to determine the amount of subarachnoid and intraventricular hemorrhage to predict vasospasm and clinical outcome.[70] Because

of the importance of these prognostic factors, improved prevention and treatment of the subsequent complications from SAH can only improve the prognosis to a limited extent.[133]

According to clinical guidelines, SAH patients should be treated in high-volume institutions, managing at least 20 cases annually.[29] However, a Scandinavian study found no association between treatment volume and 1-year outcome after SAH.[99]

Most patients with subarachnoid hemorrhage need long-time care. During and after hospital admission, rehabilitation is often multidisciplinary, involving physical, occupational and speech therapies, as well as neuropsychological evaluation.[149] One year after the incident, 50 % of SAH survivors have sequelae. In a study from Australia and New Zealand, 46% reported ongoing problems with memory and mood, 14% problems with speech, and 10% with self-care.[61]

5.3 Intracranial aneurysms

The types of intracranial aneurysms are classified according to etiology (traumatic, infectious, or spontaneous) and morphology (saccular and fusiform). Traumatic aneurysms may develop secondary to penetrating trauma and skull fractures, and are often not true aneurysms, but dissections or pseudoaneurysms with missing layers of the artery wall.[158] Infectious (or 'mycotic') aneurysms can arise because of bacteremia, and most commonly from infected emboli due to infective endocarditis.[122,179]

Fusiform aneurysms may form in part because of atherosclerosis, and consist of dilatation of the entire circumference of the involved vessel.

Saccular aneurysms (or 'berry' aneurysms), the subject of this thesis, are thin-walled protrusions from the intracranial arteries.

5.3.1 Pathogenesis

Normal blood vessel walls consist of three layers. From inside to outside, these are; a) the tunica intima with the basal membrane and endothelial cells, b) the tunica media with vascular smooth muscle cells, and c) the tunica adventitia mainly consisting of collagen, providing structural integrity of the vessel wall. An internal elastic lamina separates tunica intima and tunica media, and an external elastic lamina separates tunica media and tunica adventitia.[38]

Cerebral arteries have structural differences from extracranial arteries that can contribute to aneurysm formation. The tunica adventitia is sparse, the proportion of elastic fibers is lower, and cerebral arteries are immersed in cerebrospinal fluid instead of supportive connective tissue.[39,40,89]

IAs are acquired lesions. A focal damage in the vascular wall resulting from hemodynamic stress is the most likely direct cause of aneurysm formation.[22] Bifurcations and the outer lateral wall of vessel bends are exposed to abnormally high levels of hemodynamic stress and are predilection sites for aneurysms.[62] Anatomical variations in the circle of Willis leading to increased hemodynamic stress are also considered important factors in IA formation.[40,89,97]

The wall shear stress (WSS) is a frictional force generated by blood flowing past the apical surface of endothelial cells. Intracellularly, this mechanical stress is converted into biological signals. The signals act both directly by modulating cellular functions such as adhesion molecules, integrins and ion canals, and indirectly by regulating gene expression.[94,141] Abnormally high or low WSS disrupts the vessel wall.[25] High WSS causes mechanical wear that exceeds the strength of the wall. Too low WSS levels reduce mechanobiological proliferation signals, leading to degeneration of endothelial cells through apoptosis.[141] High WSS initiates aneurysm formation, but whether high or low high or low WSS is most relevant for further growth and weakening of an aneurysm remains unclear, and has spurred considerable debate.[77,108]

Figure 5 illustrates structural and ultrastructural components of IAs. The most common histological findings of aneurysm walls are inhomogenous walls with a disrupted internal elastic lamina, disintegrated endothelium, and a thinned tunica media containing few smooth muscle cells. The finding of inflammatory cells is a hallmark.[62]

Disruption of the internal elastic lamina causes mechanical overload on the vessel wall. In response, the vascular smooth muscle undergo phenotype modulation from contractile units to cells that synthesize collagen matrix, and eventually to dedifferentiated, proinflammatory smooth muscle cells.[23] Sustained mechanical overload will cause inflammatory responses to be the main drivers of aneurysm formation. These responses are mediated by inflammatory cytokines such as tumor necrosis factor (TNF), IL-1β and matrix metalloproteinases (MMPs), causing influx of macrophages and continuous degradation of collagen and elastin fibres.[23,40,49,54]

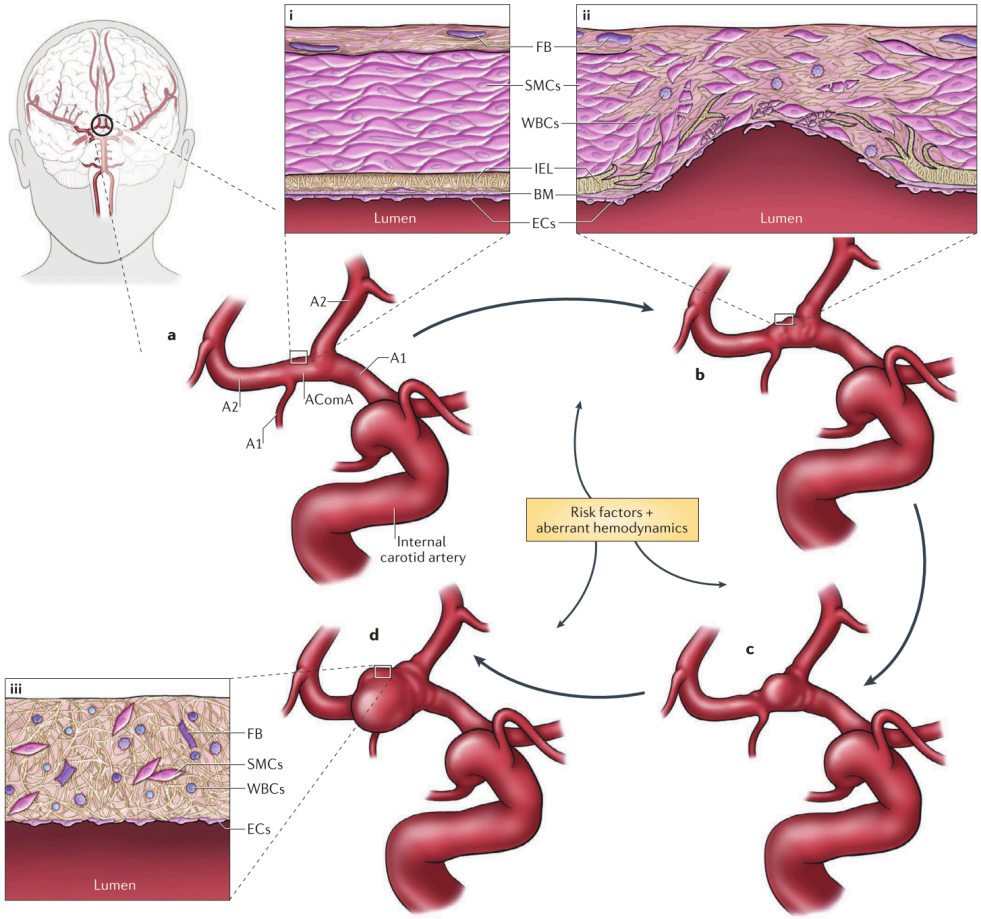

Figure 5. Structural and molecular pathogenesis of intracranial aneurysm.

*Panel **a** illustrates the anterior communicating artery (ACoA) complex, filling from the left (dominant) anterior cerebral artery (A1) and, to a lesser extent, from the hypoplastic right A1 — a variation typically found in ACoA aneurysms. Inset **i** shows the ultrastructural composition of a cerebral artery. Panel **b** and inset **ii** shows structural changes in the wall of cerebral arteries in response to aberrant flow combined with risk factors. The detrimental processes acting on the artery wall are exacerbated by cellular and humoral inflammatory responses. Blood inflow and impingement exposes the structurally defected arterial to high wall shear stress, resulting in aneurysm sac formation (panel **c**). The aneurysmal sac continues to grow until ongoing vessel wall repair and extracellular matrix degradation reach a balance (panel **d**). The main molecular constituent of the aneurysm wall is collagen (inset **iii**). The main cellular components in the aneurysm wall are SMCs, a discontinuous layer of ECs and a minor proportion of inflammatory cells, such as macrophages, neutrophils and lymphocytes.*

*BM, basement membrane; EC, endothelial cells; FB, fibroblast; IEL, internal elastic lamina; SMC, smooth muscle cell; WBC, white blood cell. Reprinted by permission from Macmillan Publishers Ltd: Etminan N, Rinkel GJ. Unruptured intracranial aneurysms: development, rupture and preventive management. **Nat Rev Neurol 12**:699–713, 2016, copyright 2016.*

Aneurysm growth is discontinuous and stochastic rather than linear. This is clarified through both mathematical simulations,[80,137] molecular analysis of human aneurysms,[39] and repeated radiological imaging of aneurysms.[14,172] Some aneurysms remain stable and unchanged for years, others develop and rupture within weeks or months, and longtime stability can be followed by rapid change.[40] Radiologically detectable changes are macroscopic manifestations of underlying microscopic

processes. Therefore, any detected morphologic change should be interpreted as a sign of aneurysm wall instability, representing a markedly increased rupture risk.[40,107,137,172]

The rupture of an IA occurs when wall tension exceeds the aneurysm wall strength.[8] As described by the Law of Laplace (see section 5.4.2.1), as the radius of an aneurysm increases compared to its parent vessel, the aneurysm wall needs a higher wall tension to tolerate increases in transmural pressure (see section 5.4.2.1).[30] Also, through the mechanisms described above, the vessel wall can be severely weakened and able to withstand less transmural pressure than under normal conditions.[23]

5.3.2 Clinical presentation and diagnosis

IAs are usually asymptomatic. Estimates are unceratin, but around 15% may experience symptoms.[51] Symptoms include third cranial nerve palsy (particularly posterior communicating artery [PCoA] aneurysms), visual acuity loss or ophthalmoplegia, headache, symptoms of mass effect, and ischemia owing to emboli originating from within the aneurysm.[51,129]

Most aneurysms are detected either upon rupture, or incidentally. Unruptured IAs are increasingly being discovered because of the extended availability and use of CT and MRI.[19,170,173]

As with SAH, the three main diagnostic modalities to investigate IAs are DSA, CTA and MRA. Patients with unruptured IA are often otherwise healthy, and emphasis is on choosing options associated with low risk. CTA is the fastest option, and less invasive than DSA because only intravenous contrast is needed. MRA takes considerably longer to perform, but is often the preferred option for follow-up imaging because it is noninvasive and without radiation.[18,93]

5.3.3 Natural history and risk of rupture

Knowledge about the natural history and risk of rupture of unruptured IA is sparse, because most aneurysms are asymptomatic or treated during follow-up. Also, the available studies on unruptured aneurysms can be flawed by selection biases and relatively short follow-up time.[82,147]

The largest original studies to date are the International Study of Unruptured Intracranial Aneurysms (ISUIA)[67,173] and the Unruptured Cerebral Aneurysm Study of Japan (UCAS Japan).[68] Though the studies were large, a large proportion of the patients were eventually selected for treatment (32% and 48%, respectively), and follow-up was short (mean follow-up time 4.1 and 1.7 years, respectively).[82] Though many unruptured aneurysms are stable during the first years of follow-up, the risk of growth is large over time. In a pooled analysis of four studies, 25% of aneurysms had grown after 9 years, and 45% after 19 years.[40] Therefore, results from studies with short follow-up time cannot be extrapolated to make long-term predictions about aneurysm stability and risk of rupture.[80]

The PHASES (population, hypertension, age, size of aneurysm, earlier SAH from another aneurysm, site of aneurysm) score was derived from a meta-analysis of studies on IA natural history to establish the risk of rupture. The ISUIA and UCAS Japan studies comprise 74% of the patients with SAH in the PHASES meta-analysis, and many limitations are therefore shared between these studies.

The largest long-time study of unruptured aneurysms comes from a Finnish cohort of 118 patients followed until death or SAH (mean follow-up time of 18.5 years). 29% of the included patients experienced aneurysm rupture during follow-up, and the annual rate of rupture was 1.6%. This rupture rate may be higher than in the general population because 93% of the study subjects had previous SAH from another aneurysm. Still, the results suggest that a substantial proportion of patients with IAs will experience SAH during their lifetime if the aneurysm is not treated.[83]

Specific risk factors for rupture can be divided into factors mostly related to the patient as a whole, and factors related to the aneurysm in particular.

5.3.3.1 Patient-related risk factors

The patient-related risk factors for rupture overlap with the general risk factors for aSAH (see section 5.2.1.2). These are central for the evaluation of rupture risk, but are prevalent in a large proportion of the population, and therefore insufficient to guide treatment decisions for individual aneurysms.

5.3.3.2 Aneurysm-related risk factors

The most studied aneurysm-related risk factors for rupture are size, location and growth during follow-up. Recent studies have focused on a more precise description of the aneurysm morphology, as well as intra-aneurysmal blood flow. This area of research will be considered in section 5.4.

Aneurysm size is the most powerful risk factor. In a meta-analysis of six prospective cohort studies with <5 mm as reference size, hazard ratios for 5.0-6.9, 7.0-9.9, 10.0-19.9 and ≥22.0 were 1.1, 2.3, 5.5 and 20.8, respectively.[59] The ISUIA study sparked considerable debate when it found a rupture rate of 0% among aneurysms <7 mm in the anterior circulation.[173] The finding was probably falsely low due to selection bias.[72,74] Since then, several studies have established that the majority of aSAH is caused by small aneurysms.[48,52,72,140] In a recent case series, aneurysms <5 mm accounted for 50% of aSAH from 2012 to 2016.[10]

Aneurysms located on the anterior communicating artery (ACoA), PCoA and the basilar apex have the highest risk of rupture, with a hazard ratio of around 2.0 compared to aneurysms on the middle cerebral artery (MCA). Internal carotid artery aneurysms (ICA) have a much lower risk of rupture (hazard ratio, 0.5).[10,59]

Aneurysm growth is a strong risk factor for rupture,[4,17,27,154,168] possibly increasing risk 12- to 24-fold.[17,154] Growth rate and risk of growth increases with increased aneurysm size, but growth can occur at all aneurysm sizes.[3] Also, though as much as 90% of aneurysms may grow before rupture, rupture can occur without growth.[14,27]

5.3.4 Treatment options

The techniques for repair of unruptured aneurysms are the same as for ruptured aneurysms, described in section 5.2.3.1. Data on safety and efficacy from randomized controlled trials on ruptured aneurysm repair cannot be extrapolated to the management of unruptured aneurysms. Naturally, mortality and morbidity is much higher for ruptured aneurysm repair, and risk factors may be different.[40]

Surgical repair of unruptured IAs is associated with a mortality of 1.7% and an overall morbidity (including death) of 6.7%, according to a meta-analysis from 2013 of 60 studies with 9,845 patients. The validity of the data is limited because the majority of the studies were retrospective or single-center studies lacking predefined outcome measures or independent and blinded end point analysis. A third of the studies reported obliteration rates: 92% of repaired IAs were completely occluded, 4% had neck remnants, and 4% were incompletely occluded. During follow-up after aneurysm repair, hemorrhage incidence was 0.4%. Posterior location of the aneurysm, larger diameter, and age >55 years increased the risk of unfavorable outcome after surgical repair.[40,88]

Endovascular repair might be associated with less immediate risk than surgery, but slightly higher rates of aneurysm recurrence.[109,147] A meta-analysis from 2010 of 71 studies with 5,044 patients found a mortality of 1.9% and overall morbidity (including death) of 4.8%. Studies conducted after 2004 reported lower morbidity than older studies. Complete occlusion or neck remnant occlusion was found in 86% of aneurysms, but aneurysm recurrence was detected in 24% of patients during the mean follow-up times of 0.4-3.2 years of the included studies. The annual risk of hemorrhage after endovascular repair was 0.2%.[115] Posterior location of the aneurysm, larger aneurysm size and patient age >52 years increased risk of a poor outcome. The use of additional endovascular devices, such as balloon-assisted coiling, stent-assisted coiling, and flow-diverting stents, was associated with higher rates of unfavorable outcomes (7%, 9% and 12%, respectively). However, the increased complication rates might reflect that these devices make it possible to treat aneurysms that otherwise would be ineligible for treatment.[40,114]

Operator experience is probably more directly associated with outcome after treatment for unruptured aneurysms than for ruptured aneurysms, and only medium- to high-volume institutions (>20 cases annually) are advised to perform surgical and endovascular procedures on unruptured IAs.[99,131,155]

Morbidity from both surgical and endovascular treatment has been significantly reduced the last decades.[28]

5.3.4.1 Risk of rupture versus risk of treatment

Factors affecting the management of unruptured aneurysms include life expectancy of the patient, the estimated risk of rupture, treatment risk, and also the level of anxiety caused by the awareness of having an unruptured aneurysm.[40] In an international effort to quantify and weigh the risks associated with treatment versus risk of rupture, 69 specialists developed the Unruptured Intracranial Aneurysm Treatment Score (UIATS). This is consensus-based score with a low evidence level, but can serve as a valuable tool for indicating how a large group of specialists might manage an individual aneurysm patient.[37,130]

Due to the substantial life-time risk of rupture,[83] some researchers suggest preventive treatment of unruptured aneurysms in patients <50 years irrespective of aneurysm size, provided there are no contraindications for treatment.[73] If a patient is selected for conservative management, a follow-up with MRA or CTA at 6 to 12 months after initial discovery is recommended, with subsequent follow-up every or every other year. If aneurysm enlargement is discovered, treatment should be offered unless contraindications are present.[155]

While the aSAH incidence has been stable the last decades (see section 5.2.1), the proportion of small aneurysms among ruptured aneurysms is increasing.[10] This may be due to the detection and treatment of large unruptured aneurysms.[10] Treatment decisions for patients with smaller aneurysms can be challenging. While aneurysm size is a powerful predictor for aneurysm rupture at the population level, rupture prediction at the individual level is more complex. Indeed, on a population level, the most cost-effective management of aneurysms smaller than 3 mm is no preventive treatment or follow-up imaging.[71,105] To reduce the aSAH burden also from small aneurysms, there is a need for developing predictive models to assess individual risk.

5.4 Patient-specific rupture prediction

The growing numbers of incidentally discovered aneurysms represent a challenge: because the natural history and risk of rupture is unclear, we risk over- or undertreating patients.[82] However, it also represents an opportunity. The prognosis after aSAH is largely determined already before the patient reaches hospital (see section 5.2.3.3).[133] Therefore, identifying the dangerous aneurysms beforehand

and securing them from future rupture is the management strategy with the highest potential of reducing mortality and morbidity from aSAH.

Aneurysm morphology and intraaneurysmal hemodynamics are two promising areas of research on patient-specific rupture prediction. Morphological assessment aims to describe the size, shape and configuration of the aneurysm. Evaluation of intraaneurysmal hemodynamics aims to calculate and visualize characteristics and patterns of the blood flow.

5.4.1 Morphology of intracranial aneurysms

Assessment of aneurysm morphology can be done either on cerebral angiography images, or on computerized models of the cerebral vasculature. There is a substantial heterogeneity in how researchers define and measure the different morphological parameters,[90] but parameters can be divided into 1-, 2- and 3-dimensional measurements, as well as considerations of the general appearance of the aneurysm.[178] This section gives an overview of morphological parameters, but without a detailed discussion of the different ways of defining each parameter.

1-dimensional parameters that are commonly measured include the aneurysm's maximal diameter, the diameter of the neck, and the distance from the neck plane to various locations on the aneurysm wall. Also, the aneurysm's diameter can be measured orthogonal to other parameters, such as maximal diameter orthogonal to aneurysm height.[178]

2-dimensional parameters include geometrical indices, and angles. The aspect ratio of an aneurysm is defined as the ratio between aneurysm height and neck diameter, the bottleneck factor as the ratio between width and neck diameter, and the size ratio as the ratio between height and the diameter of the parent artery from which the aneurysm arises.[32,178] Angles are measured between the flow direction of the parent artery and the direction of the aneurysm.[178]

3-dimensional parameters include volume and other parameters that take into account the 3-dimensional configuration of an aneurysm. Volume is either measured on 3-dimensional models or calculated using mathematical formulas. Volume can be included in geometrical indices, such as volume-to-neck ratio, undulation index, ellipticity index and non-sphericity index. The indices vary from 0, being a completely smooth or spherical shape, to 1. Undulation index increases when the surface becomes more irregular and when more concavities are present. Ellipticity index increases when the aneurysm is more elongated. Non-sphericity index reflects ellipticity index and undulation index, and measures the deviation of the aneurysm from a perfect sphere.[178] Finally, the writhe number has been introduced as another estimate of surface irregularity. The writhe number measures the

twisting or curving of a coil around itself, and increases when more torsional forces are applied to the aneurysm surface.[92,178]

Qualitative evaluation involves characterizing the aneurysm appearance as smooth or irregular, and counting number of blebs, which are irregular protrusions of the aneurysm wall.[150,178]

Many morphological parameters are readily available from cerebral angiographies. In 2-dimensional DSA, the viewer cannot decide the viewing angle, and measurements rely on the available viewing plane. Angiograms can be segmented into 3-dimensional models. Segmentation involves partitioning an image into sets of pixels (or voxels for volume images), based on detecting intensity and texture, edges, or geometric models.[45] Segmentation into 3-dimensional computer models allows for precise measurements, but depends heavily on the quality and resolution of the original angiography.[40,112]

5.4.2 Biomechanics and hemodynamics of intracranial aneurysms

Biomechanics is the study of structure and function of biological systems using the methods of mechanics. A subfield of biomechanics—and the focus of this thesis—is *hemodynamics*, which is concerned with the mechanical laws governing the motion of blood through blood vessels.[63]

5.4.2.1 The mechanical laws of blood flow

Blood flow through the cardiovascular system constantly exerts two pulsatile forces on the vessel walls: *cyclic pressure* and *wall shear stress*. The cyclic pressure mechanically distends the vessel wall. The wall shear stress (WSS) is a frictional force generated by blood flowing past the apical surface of endothelial cells, as described in section 5.3.1.

Pressure is a measure of compression forces. In a stagnant fluid, pressure is uniformly distributed. In solid bodies, pressure might be non-uniformly distributed due to structural irregularities.[126]

The vascular wall experiences the forces acting upon it as *stress*, a measure of the internal forces in the wall, illustrated in Figure 6. If the wall were only an infinitely thin surface, its stress would be sufficiently described by the two forces exerted by the blood flow—the cyclic pressure and the wall shear stress. However, the biological vessel wall has a certain thickness and structural integrity. Therefore, the stress experienced by the wall has many components. In addition to friction between blood and the wall (the shear stress) the components are:

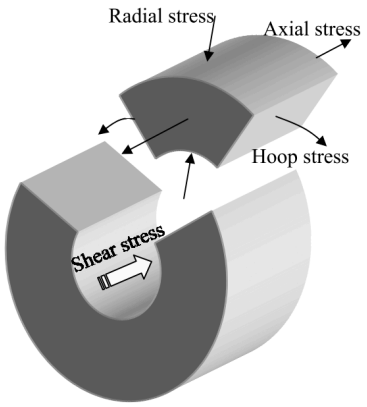

Figure 6. Stress components in a cylinder under pressure and flow. Reprinted from Raghavan ML, Kratzberg JA, Golzarian J: Introduction to biomechanics related to endovascular repair of abdominal aortic aneurysm. ***Tech Vasc Interv Radiol 8****:50–55, 2005, with permission from Elsevier.*

- hoop stress, a pressure induced force, pulling on every particle of the wall in the circumferential direction;
- axial stress, a pulling force within the wall, parallel to the vessel direction, arising when shear stress propagates through the wall;
- radial stress, a pushing force orthogonal to both the direction and the radius of the vessel.[126]

An alternative to hoop stress in describing the circumferential stress is *wall tension*. The Law of Laplace describes that there is an equilibrium between the transmural pressure and wall tension, and that the wall tension increases with the pressure and the radius. The Law of Laplace is defined as

$T = \Delta Pr$ for a cylinder, and

$T = \Delta Pr/2$ for spheres,

where T denotes wall tension; ΔP, transmural pressure; r, radius.[15]

However, the Law of Laplace assumes an infinitesimally thin wall, where the radius is at least 10 to 20 times the wall thickness. This condition is rarely met in biological vessels, and the stresses within the wall can have significant spatial variations.[30]

The nature of fluid flow can be described as a spectrum from *laminar* to *turbulent*. In laminar flow, the blood is organized in layers flowing on top of each other in a steady manner. Viscosity is the friction between adjacent layers.[161] The most central layers of flow have a higher velocity than the outermost ones. Reynolds number (Re) is a dimensionless number quantifying the relative importance of inertial forces to viscous forces. At low Re, viscous forces are dominant and the flow is laminar. At high Re, inertial forces dominate over viscous, and shear in the main flow causes turbulence and chaos. The value of Re at which a transition from laminar to turbulent flow occurs, is called the 'critical Reynolds number'.[167] In rigid pipes with steady flow, this number is 2300. Under pulsatile

conditions, as in the human cardiovascular system, the critical Reynolds numbers is substantially reduced. That is because decelerations increase the likelihood of flow destabilization. The average Reynolds number where transition flow occurred in a study of five carotid arteries, was 500. Turbulence increases the magnitude and variability of WSS.[159,161]

Exact measurement of WSS *in vivo* is almost impossible, and it is therefore investigated using computational simulation of models derived from angiographic data.[112] These simulations can also calculate flow patterns, impingement zones and velocities.[40]

5.4.2.2 Computer simulation technology applied on intracranial aneurysm hemodynamics

Computational fluid dynamics (CFD) is a well-established tool used in engineering, including aircraft and vehicles. CFD is a branch of fluid mechanics, using differential equations to simulate fluid flow. There is increasing interest in applying the technique in cardiovascular medicine. The construction and solution of a CFD model can be described in seven stages (a simplified process is shown in Figure 7):[112]

1. Clinical imaging: CTA, MRA or DSA with sufficient anatomical and physiological detail and quality.
2. Segmentation and reconstruction: Segmentation methods convert areas of interest on medical images, such as blood vessels, to geometrical models.
3. Meshing: The geometrical model is divided into discrete volumetric elements or cells. The calculations performed during the simulation are solved for each of these elements.
4. Boundary conditions and definition of fluid properties: Specifications of the physiological properties at the inlet, the outlet and the walls, and the blood density and viscosity.
5. Simulation: Calculations of Navier-Stokes and continuity equations for each volumetric element. A typical simulation is run over several cardiac cycles, each divided into hundreds or thousands of individual time-steps. Millions of non-linear partial differential equations are solved simultaneously at all time-steps, and 3-dimensional CFD modelling is therefore time-consuming and computationally demanding.
6. Post-processing: Extracting and displaying the relevant data.
7. Validation: Modelled results must be validated against other measurements to ensure an accurate and reliable model.

The CFD model relies on several assumptions, including the following:

- The walls are assumed rigid and homogenous, when in reality they are flexible and multilayered. Rigid walls may overestimate the WSS magnitude and sometimes display a different distribution of WSS than in more advanced models with flexible walls.[9] In addition to the shear stress and flow patterns, cyclic pressure is sensed by the deeper smooth muscle cells of the vascular wall. This mechanotransduction also contributes to wall maintenance, but is undercommunicated in many computational studies.[7,156] However, simulations with flexible walls require more complex computational models, are much more computationally demanding, and also introduce new assumptions and increased uncertainty.[56]
- In vivo, blood behaves as a non-Newtonian shear-thinning fluid, because red blood cells are suspended in fluid. That is, the viscosity decreases with higher velocity and shear. However, these effects are thought to have little effect in large arterial blood flow modelling, such as in the circle of Willis.[41,148]
- Laminar flow is usually assumed in cerebral aneurysms, due to the Reynolds numbers being far lower than the transitional threshold. Though the pulsatile nature of the flow and the complex geometry of vessels and aneurysms might significantly alter this critical threshold,[35,46] most studies still assume laminar flow because more complex calculations would require patient-specific velocities and waveforms.[162]

Because of the assumptions required in computational simulations, the aim should be improved understanding rather than exact numbers. Still, the ability to compute otherwise unmeasurable hemodynamic variables is valuable, and CFD has potential to greatly enhance diagnostic assessment, and design of devices such as stents.[112]

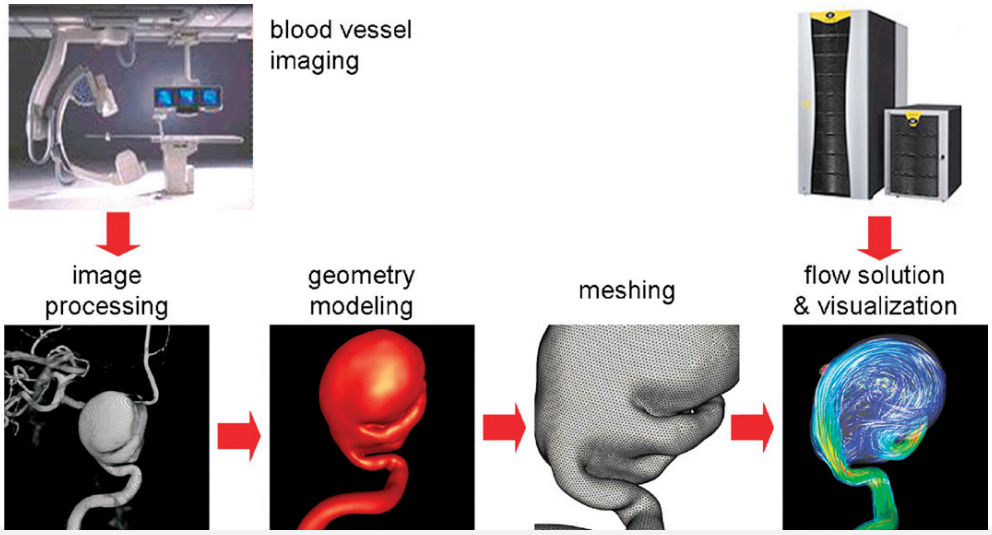

Figure 7. Image-based CFD modeling pipeline. The main steps followed to construct patient-specific computational fluid dynamics models of blood flows in cerebral aneurysms from medical images are the following: vascular modeling, blood flow modeling and flow visualization. Reproduced with permission from Cebral J, Mut F, Sforza D, Lohner R, Scrivano E, Lylyk P, et al: Clinical Application of Image-Based CFD for Cerebral Aneurysms. ***Int j Numer method biomed eng 27****:977–992, 2011.*

5.4.3 Can the morphology and hemodynamics of ruptured aneurysms predict rupture of unruptured aneurysms?

Data on unruptured IA followed until rupture is rare. Therefore, the majority of existing studies aimed to find rupture predictors compare morphology and hemodynamics from ruptured aneurysms with other unruptured aneurysm.[40]

Numerous studies have shown statistically significant morphological and hemodynamic differences between ruptured and unruptured aneurysms.[66,79,178] However, applying results from these studies on unruptured aneurysms to determine their risk of rupture critically relies on the premise that postrupture morphology is not significantly different from that prior to rupture.[40,178] Recent research indicates that this assumption does not hold. The morphology of many aneurysms changes during growth,[168,181] and case reports and small studies with 1 to 13 aneurysms indicate that morphology may change considerably around the time of rupture.[81,127,138,177]

6 Aims of the thesis

The general aim of the thesis was to improve the rupture prediction of unruptured intracranial aneurysms, based on parameters of morphology and intraaneurysmal hemodynamics. Specifically, we aimed to:

I. Compare aneurysm morphology from angiograms obtained before and just after rupture and to evaluate whether postrupture morphology is an adequate surrogate for the prerupture morphology in the evaluation of rupture risk.

II. Identify possible hemodynamic parameters at the time of diagnosis of intracranial aneurysms that are associated with future rupture.

III. Identify possible morphological parameters at the time of diagnosis of intracranial aneurysms that are associated with future rupture.

7 Methods

All studies were approved by the Northern Norway Regional Committee for Medical Research Ethics, which decided the studies to be exempt from patient consent. The studies were reported according to the Strengthening the Reporting of Observational Studies in Epidemiology (STROBE) statement for observational studies.[171]

7.1 Papers I, II and III: Electronic health records and imaging

The basis of the thesis is a nationwide retrospective data collection from the four neurosurgical centers treating all IA and SAH in Norway: The University Hospital of Northern Norway, Tromsø; St. Olav's Hospital, Trondheim; Haukeland University Hospital, Bergen; and Oslo University Hospital Rikshospitalet, Oslo. Thus, the data collection covered entire population of Norway (5,000,000 people).

We identified patients and collected clinical information from electronic health records, and retrieved cerebral angiograms.

7.1.1 Electronic health records

We searched electronic health records using codes from the *International Classification of Diseases*, version 10, to identify patients diagnosed with unruptured IA who later were hospitalized with SAH. We created lists of patients diagnosed with I67.1 (cerebral aneurysm, unruptured) between October 1, 2003, and October 1, 2013. Of these patients, we identified those being subsequently hospitalized with I60.0–I60.9 (nontraumatic SAH).

In Papers II and III, each case was matched to two controls that did not experience IA rupture during the observation period, and that neither underwent prophylactic treatment (codes AAC00, AC10, AAC15, AAL00 and AAL99 in the Nordic Medico-Statistical Committee Classification of Surgical Procedures [NCSP]). The primary matching factor was aneurysm location, and if location could not be matched, the patient was excluded. Further matching was performed in the following order: aneurysm size, patient sex and age.

For each identified patient, we recorded age, sex, date of diagnosis of unruptured IA, date admitted for SAH, and the reason for the aneurysm being conservatively managed. From the electronic health records, we also retrieved known risk factors, such as hypertension, smoking, connective tissue disease, polycystic kidney disease, family history, and prior aSAH. We determined the PHASES[59] in all patients, and UIAT[37] scores in all patients of Paper I.

7.1.2 Imaging

For Paper I, which was a case series of morphology around time of rupture, we retrieved the latest available prerupture and the first available postrupture angiograms. For Papers II and III, which were matched case-control studies of rupture predictors at time of IA diagnosis, we retrieved the first available angiograms. Figure 8 illustrates the collected angiograms in relation to time of diagnosis and rupture of the included aneurysms.

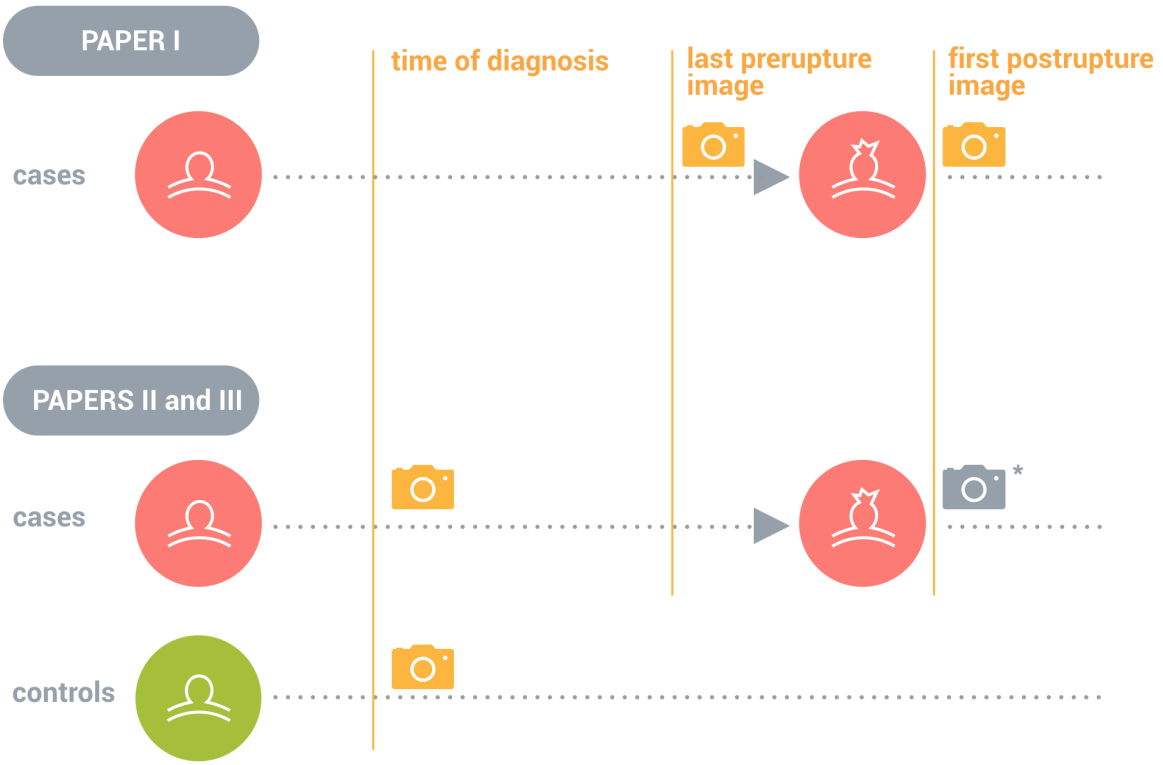

Figure 8. Collected angiograms (yellow camera symbols) in relation to the natural history of the included aneurysms. In Paper I, we compared the latest angiogram before with the first angiogram after rupture. In Papers II and III, we compared angiograms at time of diagnosis between aneurysms with and without later rupture.
**) Angiograms after rupture were also investigated in Papers II and III (grey camera symbol) to confirm the rupture of a previously diagnosed aneurysm, but these angiograms were not used in analyses.*

7.1.2.1 Diagnosis of intracranial aneurysms and subarachnoid hemorrhage

Angiograms from patients identified with the electronic health records search strategy were inspected by an experienced neuroradiologist and/or neurosurgeon to ensure the correct diagnoses. The original angiograms included DSA, CTA and MRA images (from a variety of manufacturers, because images were collected from the entire country).

Patients were excluded if they had previous treatment of the aneurysm of interest, multiple aneurysms of which the ruptured aneurysm was difficult to identify, or image quality precluding reliable aneurysm measurements. Fusiform aneurysms were excluded.

7.1.2.2 Generation of patient-specific 3-dimensional models of cerebral arteries

For Papers II and III, we generated 3-dimensional models of the patients' cerebral arteries. Segmentation into models, and the subsequent meshing and simulation in Paper II, was performed by Simula Research Laboratory, Oslo, Norway.

Segmentation of the vasculature into models and computation of the different morphological parameters were performed with the Vascular Modeling Toolkit (VMTK, http://www.vmtk.org) using the scripts vmtkbranchextractor, bifurcationreferencesystems and vmtkbranchclipper. We isolated the IA using a previously described algorithm.[123] The geometries were segmented from MRA or CTA images to include the ICA and/or basilar artery upstream of the aneurysm, and cylindrical extensions were added to both inlets and outlets. In cases where the segmentation process failed to include arteries visible on the original angiography, these arteries were created manually and attached to the segmented models.

All segmented models were inspected by an experienced neurosurgeon to ensure consistency with the original angiography. The engineering team conducting segmentation and computation was blinded to the patients' status as case or control and to any clinical data.

7.2 Papers I and III: Manual and automatic measurement of morphology

7.2.1 Manual measurement

For Paper I, two neuroradiologists performed manual measurements directly on DSA, CTA or MRA angiograms, and determined several quantitative and qualitative features of the included IA.

The two neuroradiologists resided in different centers and assessed the aneurysms using measuring tools in Siemens syngo.via and syngo InSpace (Siemens Healthcare, Erlangen, Germany). The observers measured all aneurysms independently according to the defined measurement protocol, blinded to each other's results and with no prior information about aneurysm rupture state.

Initially, the observers interactively evaluated 3-dimensional volume rendering technique images for general morphology, such as smooth/irregular and numbers of daughter sacs (Figure 9A). The

aneurysm neck was identified and multiplanar cursors were aligned to define the aneurysm neck. The aneurysm was rotated until the maximum length and diameters were revealed. The resulting volume rendering technique projection was then converted to a thin-slice maximum-intensity picture on which measurements were performed (Figure 9B).

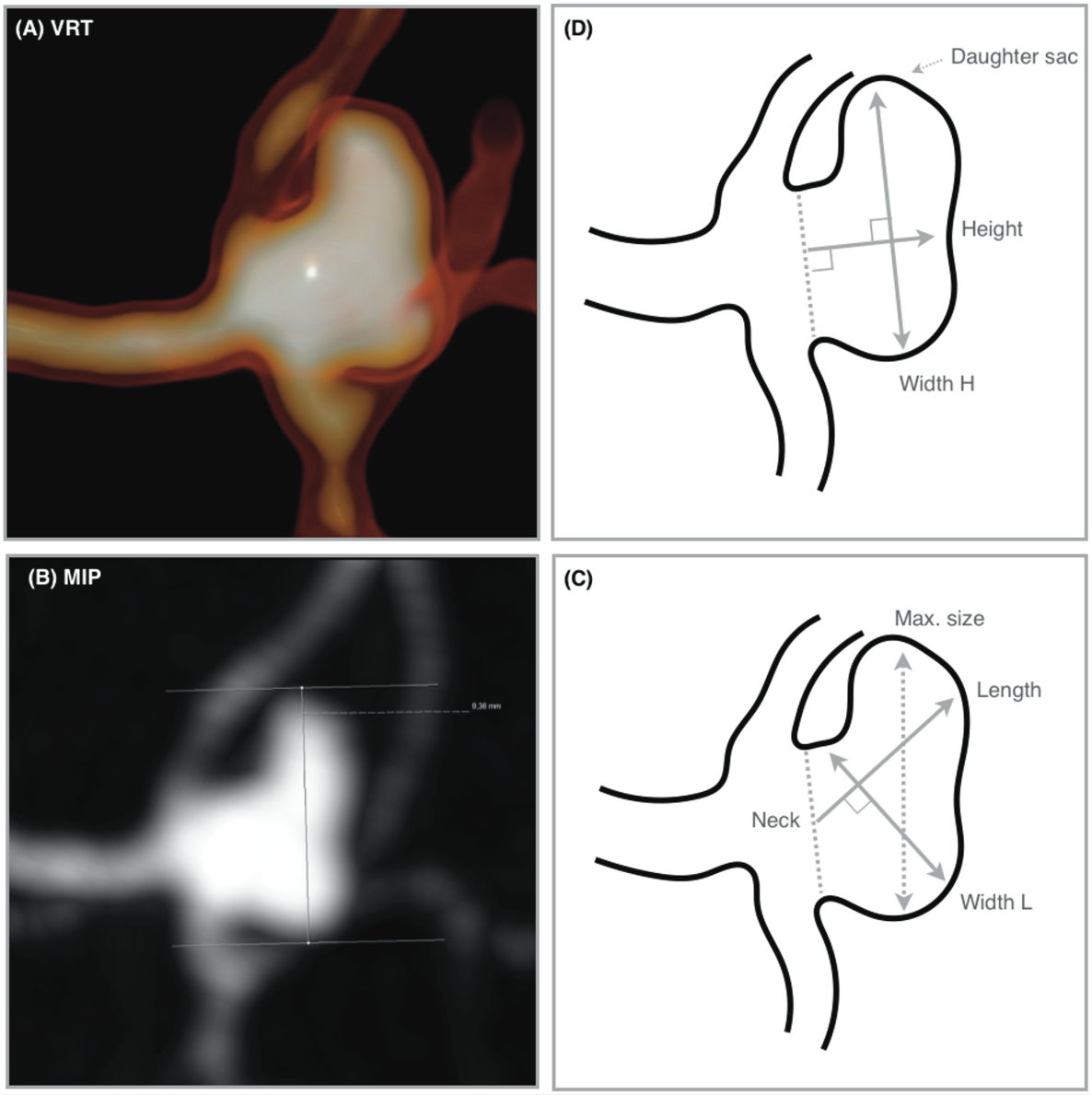

*Figure 9. Aneurysm measurement method. **A**, Volume rendering technique (VRT) image for assessment of general morphology and identification of optimal measurement planes. **B**, Maximum intensity picture (MIP) for measurements. **C** and **D**, Illustrations of parameter definitions.*

7.2.1.1 Development of measurement protocol

To ensure high reliability in the measurement process, we calculated the intraclass correlation coefficient to guide the selection of parameters.[57] According to conservative criteria, values >0.81 represent substantial reliability.[142] Mean intraclass correlation coefficient for all parameters except two was 0.88. Of the two with lower intraclass correlation coefficient, one parameter (minimal size) was excluded from further analyses, whereas the other (Neck) was redefined to increase precision. The final measurement guide is described in section 7.2.3.

The mean values between observers were chosen when interrater difference was <2 mm. In cases of ≥2 mm differences and for the redefined Neck parameter, values were settled by consensus.

7.2.2 Automatic measurement

For Paper III, automatic measurements were performed on the segmented 3-dimensional models (see section 7.1.2.2).

The automatic measurement was supplemented by a qualitative assessment of wall characteristics. One neurosurgeon and one neuroradiologist, in consensus—blinded to patients' status as case or control and to any clinical data—characterized each aneurysm as irregular or smooth based on its general appearance,[44] and counted number of blebs. Blebs were defined as "an irregular protrusion of the aneurysm wall" on cerebral angiography.[45]

7.2.3 Morphological parameter definitions

All aneurysm parameters must be fitted within the aneurysm sac. Parameter definitions were based on previous literature.[32] The definitions varied slightly between Papers I and III, because we chose definitions that were most suitable for manual and automatic measurement, respectively (Table 2). Parameters are illustrated in Figure 9, panels C and D.

Table 2. Definitions of the morphological parameter definitions used in Papers I and III.[1]

Parameters	Paper I[2]	Paper III
1-dimensional		
Maximal size	the longest line within the aneurysm	
Neck diameter	the *largest* diameter of the neck plane	the *average* diameter of the neck through the neck centroid
Height	the longest line orthogonal to the neck, *originating from the neck centroid*	as the longest line orthogonal to the neck
Length	the longest line originating from the centroid of the neck surface	
Width H	the largest diameter that is orthogonal to Height.	-
Width L	the longest line orthogonal to and intersecting the line defined by Length	
Parent artery diameter	-	the average of the artery diameter (D_1) immediately upstream of the aneurysm and $1.5 \times D_1$ upstream from this point
2-dimensional		
Aspect ratio	Height/Neck	
Size ratio	-	Length/Parent artery diameter
Bottleneck factor	Width *L*/Neck	Width/Neck
Height/Width	N/A	Length/Width
Inflow angle[3]	-	the angle between the vectors of aneurysm Length and Parent artery flow direction
3-dimensional		
Volume	$Volume = 4/3 \times \pi(A/2) \times (B/2) \times (C/2)$, where A, B, and C are maximal size, length, and width L, respectively.	automatically calculated from segmented model
Volume-to-neck ratio	-	Volume/Neck
Non-sphericity index	-	$1 - (18\pi)^{1/3} V^{2/3} / S$, where V is the aneurysm volume and S is the IA surface area
Qualitative assessment of wall characteristics		
Irregular wall	irregular or smooth, based on general appearance	
Daughter sac/bleb	irregular protrusion of the aneurysm wall	

[1]Differences between the two papers are highlighted with Italics. Dash (-) indicates that the parameter was not used for this paper.

[2]When comparing digital subtraction angiography with another image modality, the available digital subtraction angiography projections dictated which projections were used from the other modality.

[3]For anterior communicating artery (ACoA) aneurysms, which usually have two parent arteries, we used the inflow angle from the side that was most aligned with the parent artery flow direction; i.e., the side where the aneurysm Length vector was most aligned with the A1 artery flow direction vector.

7.3 Paper II: Computer simulation of hemodynamics

7.3.1 Meshing of the segmented models

The meshing was done adaptively, with the mesh being finest in the vicinity of the aneurysm, where the distance between mesh nodes are approximately 0.135 mm, increasing to approximately 0.25 mm in the remote parts of the domain. In addition, we added four boundary layers to properly resolve the velocity gradients at the wall, with a total thickness of half the average nodal distance, and a thickness factor of 0.6 between the layers. In addition, the meshing was done radius-adaptive, to ensure a sufficient resolution even in the smallest segmented vessels.

7.3.2 Simulation

We imposed a fully developed pulsatile Womersley flow profile at the model inlets, at a heart rate of 63 bpm.[65] The flow rate was scaled with the area[160] with a mean velocity of 36.5 cm/s, to obtain a mean flow rate of 245 ml/min (±100 ml/min).[65] At the outlets, we scaled the flow according to the principle of minimal work (Murray's law). In segmented models where the PCoA was not merged to the posterior circulation, we assumed zero flux.

Walls were assumed rigid and impermeable. We assumed blood to behave as a Newtonian fluid with a viscosity of 0.00345 Pa·s and a density of 1060 kg/m3.[41] The Navier-Stokes simulation equations were solved and postprocessed with the open source softwares cbcflow and cbcpost (https://bitbucket.orgsimula_cbc/), based on the open source finite element library (FEniCS).[103] The equations were solved using piecewise linear approximation of the pressure, and quadratic approximations of the velocity, effectively halving the nodal distance. The equivalent mesh sizes[162] ranged from 6.4 million to 62 million linear tetrahedral elements. To properly resolve the high frequency flow dynamics, we resolved the simulations with a temporal resolution of 0.04 milliseconds.

7.3.3 Hemodynamic parameter definitions

Table 3 (next page) specifies abbreviations, mathematical definitions and pragmatic explanations for each studied parameter. Oscillatory shear index (OSI) and low shear area (LSA) are derivatives of wall shear stress (WSS).[26] Pressure loss coefficient (PLc), inflow concentration index (ICI) and viscous dissipation rate (VDR) are related to the flow phenotype.[20,153]

7.4 Statistics

P values of <0.05 were assumed statistically significant. The variables' distribution was investigated visually with Q-Q plots and numerically with Shapiro-Wilk test. The data were analyzed with Stata for Mac (version 14; StataCorp LP, TX, USA) and SPSS for Windows (version 24; IBM, NY, USA).

7.4.1 Paper I

The variables were found to be non-parametric. Thus, continuous variables were reported as medians with range, and nominal variables as absolute numbers and percentages. Paired continuous variables were compared using Wilcoxon signed-rank test, and paired nominal variables were compared using McNemar's test. Independent continuous variables were compared using Mann–Whitney *U* test or Kruskal–Wallis test in cases of >2 groups. Categorical variables were compared using Chi-squared test.

7.4.2 Papers II and III

Parametric variables were reported as means with standard deviations (SD). Nonparametric variables were reported as medians with interquartile range (IQR). Balance between cases and controls was assessed using the Student t-test for parametric variables, and the Wilcoxon rank-sum test for nonparametric variables. Categorical variables were compared using the chi-square test.

Matched case-control analysis was performed using conditional logistic regression.[118] For multivariable regression, backward stepwise elimination of independent variables with a threshold significance level of > 0.2 was used to select the final multivariable model.

In Paper III, the relationship between Maximal Size, Size Ratio and Inflow Angle was assessed separately for cases and controls using univariate linear regression and scatterplots.

Table 3. Definitions and explanations of the studied hemodynamic parameters.

Parameter Name (Abbreviation)	Definition	Explanation
Time- and space-averaged WSS (AWSS)	$\frac{1}{A_a}\int_{\Gamma_a} \lvert\bar{\boldsymbol{\tau}}\rvert dS$	Average magnitude of the time-averaged WSS over the aneurysm wall.[21,174]
Maximum WSS (MWSS)	$\max_{x\in\Gamma_a} \lvert\bar{\boldsymbol{\tau}}\rvert$	The maximal time-averaged WSS in the aneurysm dome.[21,174]
Minimum WSS (MinWSS)	$\min_{x\in\Gamma_a} \lvert\bar{\boldsymbol{\tau}}\rvert$	The minimal time-averaged WSS in the aneurysm dome.
Logarithmic WSS (LnWSS)	$\frac{1}{A_a}\int_{\Gamma_a} \overline{\ln\lvert\boldsymbol{\tau}\rvert}\, dS$	Time-and space average logarithmic WSS magnitude over the aneurysm wall.[91]
Min. logarithmic WSS (MinLnWSS)	$\min_{x\in\Gamma_a} \overline{\ln\lvert\boldsymbol{\tau}\rvert}$	Minimal time-averaged logarithmic WSS in the aneurysm.[91]
Oscillatory shear index (OSI)	$\frac{1}{A_a}\int_{\Gamma_a} \frac{1}{2}\left(1-\frac{\lvert\bar{\boldsymbol{\tau}}\rvert}{\overline{\lvert\boldsymbol{\tau}\rvert}}\right) dS$	Measurement of the directional change of the WSS vector, averaged over the aneurysm dome.[174]
Low shear area (LSA)	$\frac{1}{A_a}\int_{\Gamma_a} \begin{cases} 1, \text{if } \lvert\bar{\boldsymbol{\tau}}\rvert < 0.1\text{AWSS}_{pa} \\ 0, \text{otherwise} \end{cases} dS$	Areas of the aneurysm wall exposed to a WSS below 10% of the mean parent arterial WSS, normalized by dome area.[174] AWSS_{pa} is computed as AWSS, over the parent artery domain.
Pressure loss coefficient (PLc)	$\overline{\left(\frac{\left(\frac{1}{2}\rho\lvert\boldsymbol{u}_{in}\rvert^2+p_{in}\right)-\left(\frac{1}{2}\rho\lvert\boldsymbol{u}_{out}\rvert^2+p_{out}\right)}{\left(\frac{1}{2}\rho\lvert\boldsymbol{u}_{in}\rvert^2\right)}\right)}$	Pressure loss associated with the aneurysm domain, relative to the kinetic energy in the parent artery.[153]
Inflow concentration index (ICI)	$\overline{\left(\frac{Q_{in}/Q_{pa}}{A_{in}/A_{neck}}\right)}$	Concentration of inflow into the aneurysm, relative to the flow rate in the parent artery.[21]
Shear concentration index (SCI)	$\overline{\left(\frac{F_h/F_a}{A_h/A_a}\right)}$	Amount of shear that is concentrated in the high-shear region of the aneurysm dome.[21]
Viscous dissipation ratio (VDR)	$\overline{\left(\frac{\frac{1}{V_a}\int_{\Omega_a} 2\nu\lvert\lvert\epsilon\rvert\rvert^2 dV}{\frac{1}{V_{nv}}\int_{\Omega_{nv}} 2\nu\lvert\lvert\epsilon\rvert\rvert^2 dV}\right)}$	Amount of energy dissipation in the aneurysm domain, relative to the energy dissipation in the near vessel domain.[21]

$\boldsymbol{\tau}$ = instantaneous wall shear stress vector; $\overline{\cdot}$ = a time-averaged quantity over one heartbeat; Γ_a = the aneurysm wall with corresponding area A_a; $|\cdot|$ = a vector magnitude; $\mathbf{u}_{in}/p_{in}$ = the velocity/pressure in the plane one diameter upstream from the aneurysm; $\mathbf{u}_{out}/p_{out}$ = the velocity/pressure in the plane one diameter downstream from the aneurysm; Q_{in} = the flow into the aneurysm; Q_{pa} = the parent artery flow rate; A_{in} = the area of inflow into the aneurysm; A_{neck} = the total neck area; A_h = the area of high shear (1 SD above the average WSS in the near vessel domain); F_h = the total shear over A_h; F_a = the total shear over the aneurysm; Ω_a = the aneurysm domain with corresponding volume V_a; Ω_{nv} = the near vessel domain (<1cm from the aneurysm) with corresponding volume V_{nv}; ν = the kinematic viscosity; ε = the strain-rate tensor; $||\cdot||$ = the Frobenius norm.

8 Results

8.1 Paper I

Title: "Cerebral Aneurysm Morphology Before and After Rupture: Nationwide Case Series of 29 Aneurysms"

The search identified 52 patients with confirmed aSAH, originating from aneurysms that were recognized but not repaired prior to rupture. Of these, 23 were excluded (9 were fusiform and 14 because of missing or poor images).

The remaining 29 patients were included in the study. Median time span between imaging prior to and just after rupture was 12 months (range, 0.3–96 months).

All 1-dimensional parameter medians were statistically significantly larger after rupture, except neck diameter. Median aspect ratio before rupture was 1.5 (range, 0.8–4.0) compared with 1.9 (range, 0.8–6.7) after rupture ($p = 0.008$). Median bottleneck factor was 1.5 (range, 0.9–4.0) before and 1.5 (range, 0.7–6.2) after rupture ($p = 0.068$). Number of aneurysms with ≥1 daughter sac was 9 (31%) before and 17 (59%) after rupture ($p = 0.005$). Figure 10 illustrates a typical change from pre- to postrupture image. The magnitude of change was clearly dependent on the time elapsed between the image prior to and just after rupture, visualized in Figure 11.

Clinical risk factors were not significantly associated with morphological change. In hypertensive patients, aneurysms were significantly larger at diagnosis. However, changes in morphology from before to after rupture were not significant, except for neck diameter, which tended to increase in hypertensive patients (0.3 mm [−1.8 to 3.7]) and decrease (−0.4 mm [−2.9 to 0.5]) in nonhypertensive patients ($p = 0.047$). Between current and former/never smokers, there was neither a significant difference in morphology prior to rupture nor a significant change in morphology after rupture.

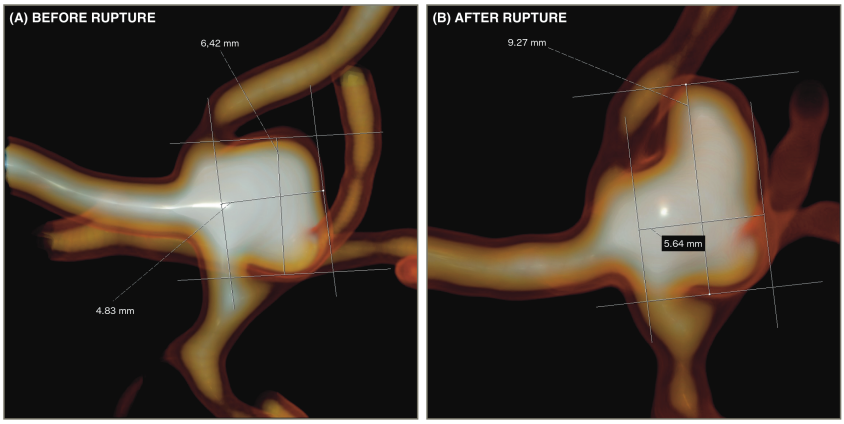

*Figure 10. Volume rendering technique (VRT) images of one aneurysm before and after rupture. Height and Maximal size measurements are shown. **A**, Before rupture. **B**, After rupture. Maximal size is increased and a daughter sac has developed.*

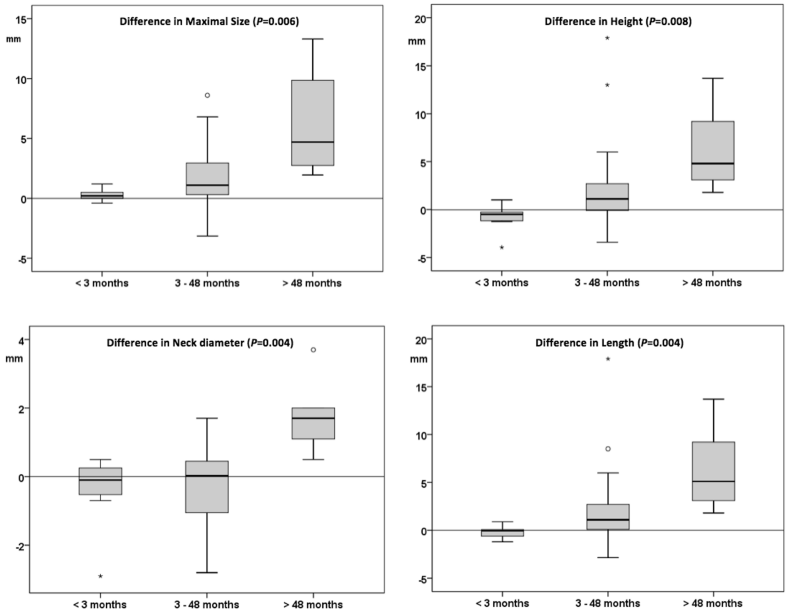

Figure 11. Difference between pre- and postrupture measurements of the 1-dimensional parameters Maximal size, Height, Neck and Length, categorized in accordance with the time elapsed between images. P values from independent samples Kruskal-Wallis test.

8.2 Paper II

Title: "Rupture prediction of intracranial aneurysms: a nationwide matched case-control study of hemodynamics at the time of diagnosis"

Of the 43 patients with confirmed aSAH, originating from saccular aneurysms that were known prior to rupture and had been treated conservatively, 20 were excluded because matching was not accomplished; of these, 18 had aneurysms larger than 10 mm. Eight cases were excluded because of insufficient image quality, and 3 were excluded because of insufficient image quality in the available controls. Each of the remaining 12 patients were successfully matched to 2 control patients with a confirmed saccular IA that was neither treated nor ruptured during follow-up.

The cases consisted of 4 ACoA, 7 MCA, and 1 PCoA aneurysms. For cases, the median time from diagnosis to rupture was 3.4 years (IQR 1.6–6.3 years). For controls, the median time from diagnosis to death or end of follow-up was 4.5 years (IQR 3.7–8.2 years).

In the univariate analysis, LSA was the only parameter statistically significantly associated with future rupture ($p = 0.041$). Minimum logarithmic WSS, averaged logarithmic WSS, PLc, and ICI showed a tendency to be associated with rupture ($p = 0.09$, 0.14, 0.15, and 0.18, respectively. Figure 12 visualizes WSS and LSA for all case and control aneurysms.

In the multivariable analysis, LSA ($\beta = 8.72$ [95% CI 0.85–16.59], $p = 0.030$) and ICI ($\beta = 1.13$ [95% CI −0.30 to 2.55], $p = 0.12$) were retained in the conditional logistic regression model. Their p values remained almost constant when adjusting for the matching variables patient sex, age, aneurysm location and size, as well as smoking status, previous SAH, hypertension, and PHASES score.

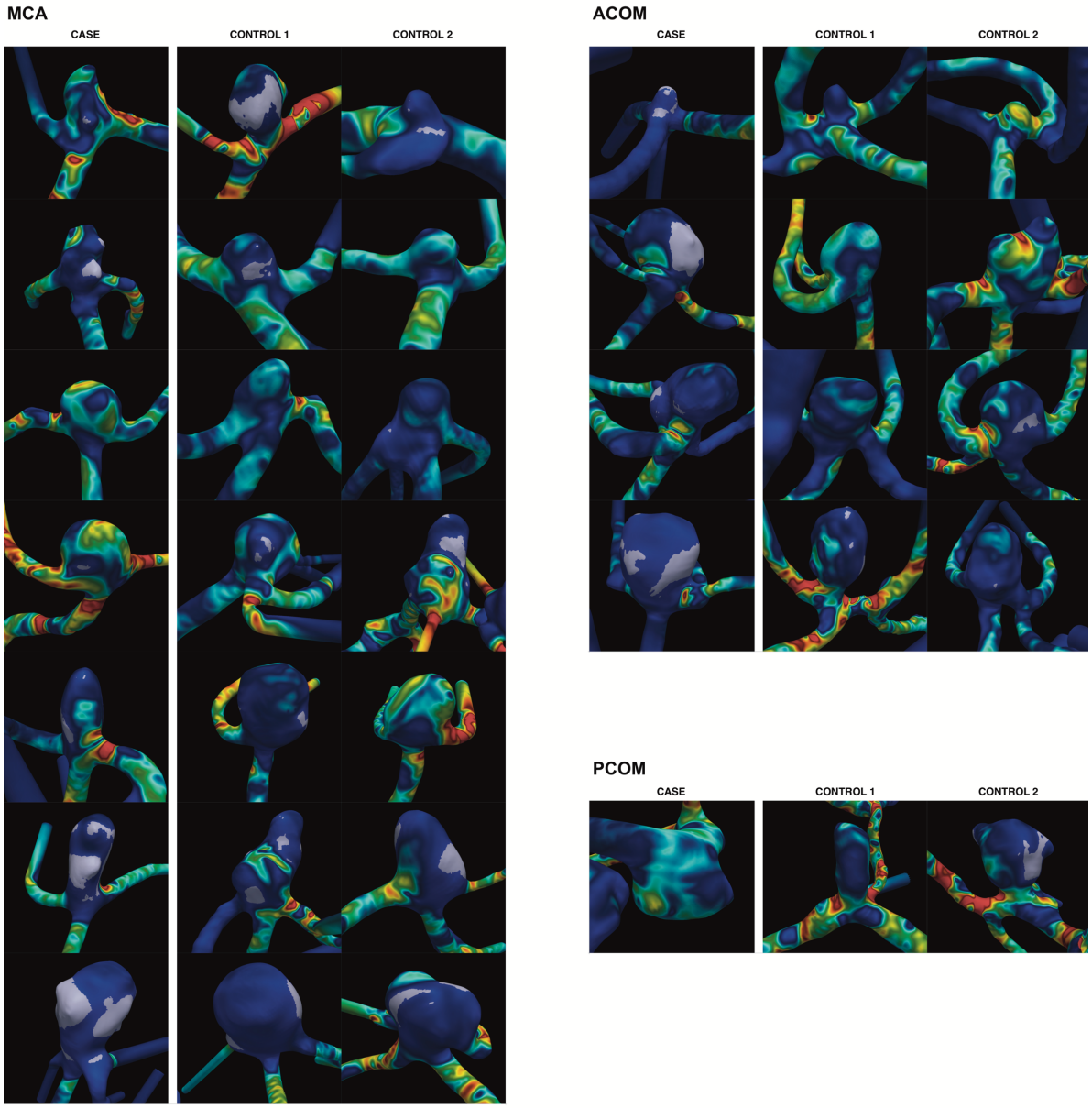

Figure 12. Visualization of WSS and LSA for all case and control aneurysms, grouped by location. The WSS is represented by a color scale ranging from blue for WSS < 1.0 Pa, to red for WSS > 10 Pa. Areas of low shear are colored gray, and represent areas of the dome where the average WSS is below 10% of the average WSS in the parent artery. ACOM = ACoA; PCOM = PCoA.

Reprinted from Skodvin TØ, Evju Ø, Helland CA, Isaksen JG: Rupture prediction of intracranial aneurysms: a nationwide matched case-control study of hemodynamics at the time of diagnosis. [E-published ahead of print] ***J Neurosurg****, 2017, with permission from American Association of Neurological Surgeons.*

8.3 Paper III

Title: *"Prerupture intracranial aneurysm morphology in predicting risk of rupture: A matched case-control study."*

The study was conducted on the same aneurysms that were included in Paper II, with 12 saccular IA patients with confirmed aSAH matched to 2 control patients with a saccular IA that was neither treated nor ruptured during follow-up.

In the univariate analysis, Inflow Angle was the only parameter that was significantly associated with future rupture. The median Inflow Angle was 19 degrees (IQR, 8-42) in cases, compared to 45 degrees (27-74) in controls ($p = 0.045$). P values for the other automatically measured parameters ranged from 0.19 to 0.89. P values for irregular wall and number of blebs were 0.22 and 0.14, respectively.

In the multivariable analysis, Inflow Angle was retained in the conditional logistic regression model (the p value, therefore, was the same as in the univariate analysis).

Figure 13 visualizes Maximal Size—one of the matching factors—in relation to Size Ratio and Inflow Angle (panels A and B, respectively). A higher Maximal Size correlated with an increased Size Ratio for both cases ($R^2 = 0.46$, $p = 0.015$) and controls ($R^2 = 0.64$, $p = <0.001$). The relation with Inflow Angle, however, was different in cases and controls. The Inflow Angle of IAs that did not rupture showed no correlation with Maximal Size ($R^2 = 0.001$, $p = .87$), whereas in IAs that later ruptured, a straighter Inflow Angle was correlated with larger maximal size ($R^2 = 0.58$, $p = 0.004$).

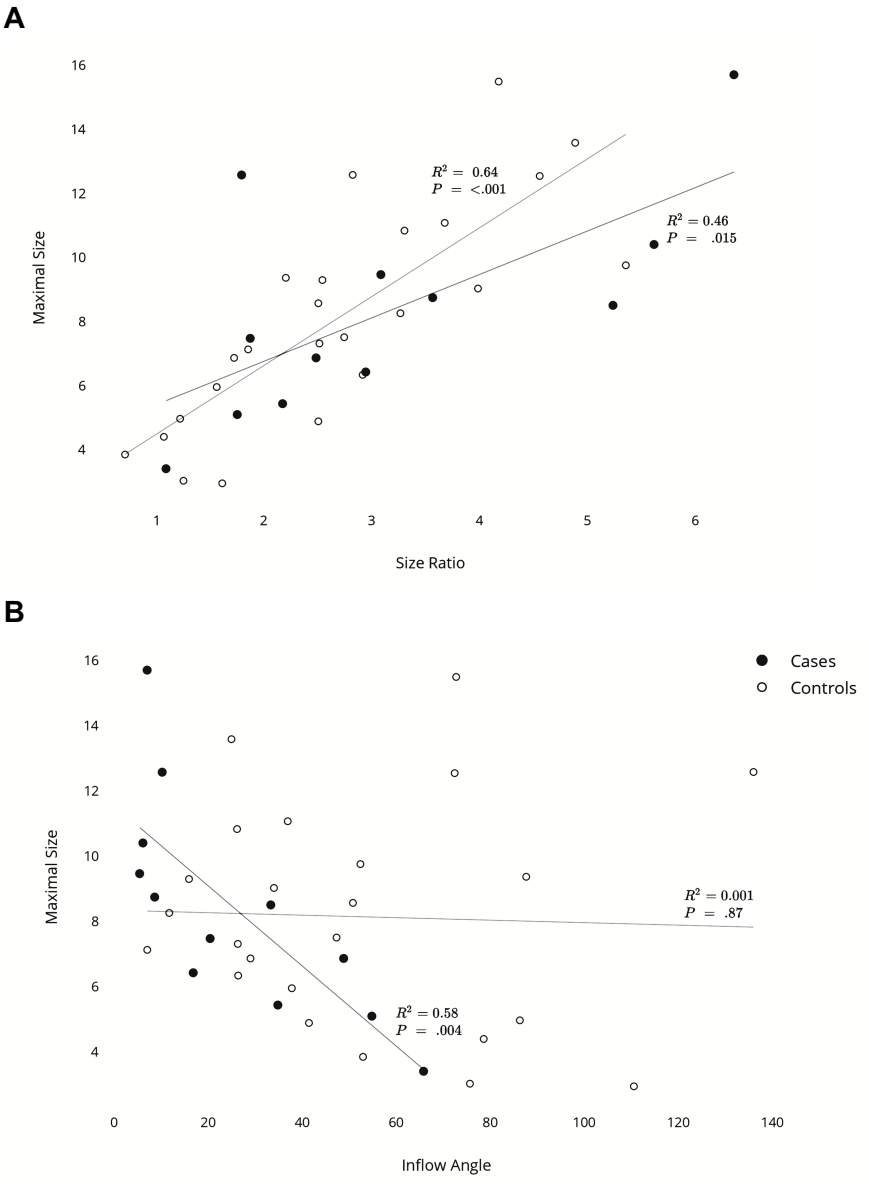

*Figure 13. Scatterplots of Maximal Size in relation to **A**, Size Ratio and **B**, Inflow Angle for cases and controls. Linear regression shown separately for cases and controls.*

*Reprinted from Skodvin TØ, Evju Ø, Sorteberg A, Isaksen JG: Prerupture intracranial aneurysm morphology in predicting risk of rupture: A matched case-control study. [Accepted] **Neurosurgery**, 2018, with permission from Oxford University Press.*

9 Discussion

There are three main findings of this thesis. First, the postrupture morphology of the intracranial aneurysms was different from the prerupture morphology. Second, hemodynamic parameters at time of diagnosis were different in aneurysms that later ruptured compared to those that did not. A larger low shear area (LSA) might be an early predictor of aneurysm rupture. Third, most morphological parameters at time of diagnosis were not different in aneurysms that later ruptured. An exception was the inflow angle, which was more parallel with the flow direction in these aneurysms.

9.1 Strengths and limitations of the study

Retrospective case-control studies and case series are placed low in the hierarchy of statistical evidence. Their use can, however, be appropriate in lack of higher-level good quality evidence.[119] Because of the devastating nature of SAH and the scarce knowledge about which IAs will rupture, a randomized trial between prophylactic and conservative treatment—or randomization to risk behavior such as smoking—is highly unethical. Moreover, SAH from known IAs are rare. Cohort studies require large numbers to be adequately powered. In this setting, case-control studies may be the source of the best possible evidence. [12]

9.1.1 Strengths

There are three main strengths of the study. First, the study provides data on unruptured IA that later ruptured, which is exceedingly rare. An answer to the question of whether the postrupture morphology can be used to assess the rupture risk of unruptured IA, addressed in paper I, has been warranted by the scientific community for decades.[40,79,178] The unique 11-digit identification number of all Norwegian citizens enabled a population-based approach to link diagnosis and procedure codes across the entire country, ensuring superior data quality compared to previous studies.

Second, the matching on both patient and aneurysmal characteristics between cases and controls in Papers II and III was pivotal to combat confounding bias. For instance, unmatched studies reporting WSS differences between ruptured and unruptured aneurysms might simply observe the effect of other factors on hemodynamics. Lauric et al. observed a strong negative correlation between WSS and aneurysm volume ($R^2 = 0.97$).[91] The importance of matching based on clinical factors is illustrated in a prospective study that estimated the joint hazard ratio for aneurysm rupture associated with smoking and hypertension to be 13.3 (95% CI 6.9–25.4).[98] The matching increases internal validity,[50] and statistical power was increased because we were able to match two controls for each case.

Third, we have selected strict parameters and strived to define them in a reproducible manner. There is a substantial heterogeneity of parameter definitions in previous literature.[90] To raise the prestudy odds of a true finding in our studies,[69] we limited the number of hemodynamic and morphological parameters, and chose only parameters that have shown association with ruptured aneurysms in previous studies.

9.1.2 Limitations

Bias, effect modification and random error might distort the association between parameters and outcome reported in the papers.[144]

9.1.2.1 Bias

Bias relates to systematic errors that result in an incorrect estimate of the association between exposure and outcome. These errors can be broadly divided into selection, information and confounding bias.

The studies of the thesis were subjected to selection bias because the included patients were selected for conservative management, except those who either refused treatment or experienced aSAH while waiting for IA repair. Thus, the IAs in the studies may have appeared less dangerous to the responsible clinicians, and we may have been unable to study rupture predictors in highly unstable and fast-growing IA. In Papers II and III, we studied characteristics of aneurysms at their first presentation. Because morphology may change over time, morphological and hemodynamic differences between cases and controls may have been larger closer to the time of rupture (see section 9.3.1.3). The matching in Papers II and III caused large IAs to be underrepresented, since patients with such aneurysms are quickly treated and not readily available as controls. However, this selection bias caused a relative emphasis on small- and moderate-sized IAs, where decision support is needed the most.

Several types of information biases affect the results. Retrospective study designs are prone to recall bias, because both clinicians and patients may report exposure differently for cases and controls. A differential information bias may affect Paper I, in which the rupture status affected IA measurements. Though the radiologists received no prior information about the rupture status, they would in many instances be able to detect which images belonged to postrupture IA. In spite of a long follow-up time, Papers II and III suffered from misclassification bias if any of the control aneurysms would eventually rupture during further follow-up. Information about blood pressure and smoking was registered in an unstructured manner in the electronic health records. Therefore, this data cannot be adequately trusted neither when present nor absent.

Confounding bias occurs when an additional (possibly hidden) variable is associated with both the exposure and the outcome, but not being on the pathway between the exposure and outcome itself.[144,152] Examples of possible confounders in the studies are intraaneurysmal thrombi and aneurysm wall composition. Thrombi might alter the flow that is depicted on the angiograms, which in turn affects measurement and simulation results. The CFD analysis assumes homogenous walls, whereas in reality the walls are multilayered and with varying thickness. Future studies can elucidate the relation between thrombi, wall composition, intraaneurysmal flow and IA rupture.

9.1.2.2 Effect modification

Effect modification exists when a variable alters the effect of an exposure on the outcome differently for different groups.[152] Previous studies have shown differences between male and female blood vessel radius and bifurcation geometry.[96] Such geometrical differences can affect both morphological and hemodynamic parameters. The proportion of men and women is unequal within the three papers, and possible effect modification cannot be excluded.

9.1.2.3 Random error, multiple testing and sample size

Random errors are evenly distributed among cases and controls, but reduce accuracy. Sources of random error include—but are not limited to—the segmentation process, assumptions related to CFD analysis (see section 5.4.2.2), variable angiogram quality, CTA and MRA slice thickness, radiocontrast filling effects, and measurement imprecision.

To measure and reduce interobserver variability in Paper I, we calculated the intraclass correlation coefficient (ICC) between the two neuroradiologists, and only used parameters that demonstrated high reliability (see section 7.2.1.1). 45% of the cases in Paper I were evaluated with different image modalities, but other studies have shown that different modalities can be reliably compared.[58]

The combination of random error with the limited sample sizes in the papers carries the risk of a statistical Type II error, in which a true difference between cases and controls is not detected.[152] This especially pertains to parameters that were present in few of the included aneurysms, such as blebs.

Multiple simultaneous hypothesis tests, such as the univariate analyses in the three papers, gives the risk of a statistical Type I error, in which a false difference between cases and controls is detected. However, one cannot know which of any significant finding is a Type I error. Methods to correct for multiple hypothesis testing, such as Bonferroni's correction, reduce the significance level. This avoids spurious significant results, but inflates the rate of Type II errors.[139]

In summary, though matching increases selection bias and therefore decreases generalizability, we believe the matched design was highly warranted to control for known confounders and effect modifiers of IA morphology and hemodynamics.[50] We cannot rule out Type I or Type II errors and must interpret our results carefully. Still, we know that research on IA around time of rupture and at time of diagnosis is clinically sought-after. Therefore, despite limitations, we consider it almost unethical *not* to publish our data, since we have had the rare opportunity to investigate prerupture aneurysms.

9.2 Aneurysm morphology before and after rupture

The core finding of Paper I was that IA morphology had changed between imaging prior to and just after aneurysm rupture. The observed changes increased with the time elapsed between imaging, though gross changes also occurred within short time spans. Change occurred in a non-uniform manner, signified by changes in aspect ratio and fraction of aneurysms with daughter sacs.

These findings did not support the assumption that postrupture morphology is representative for the prerupture morphology.[178] The fraction of IA with blebs increased from 31% before to 59% after rupture. Consistent with our study, a previous literature review reported that 17 of 23 IA increased in size around time of rupture, and a case series in the same work showed presence of new daughter sacs after rupture in 5 out of 6 patients.[177] However, in a meta-analysis including 4972 unruptured IAs, nine percent of aneurysms enlarged within a mean follow-up time of 2.8 patient-years.[5] Accordingly, our data did not reveal what occurs during the exact moment of rupture, but rather supported the notion that aneurysms grow over time, with periods with and without growth, and an inconstant risk of rupture over time.[14,27,80] IA morphology just after rupture will be shaped by the rupture per se or even in the short time span between rupture and postrupture imaging, plus any change that may have occurred along the evolution of the aneurysm.

In summary, studies comparing unruptured aneurysms with aneurysms presenting after rupture have generated important hypotheses about pathophysiology and risk factors for growth and rupture.[174] With the addition of the results from Paper I to existing data, we argue that the postrupture morphology should not be considered a good surrogate in the evaluation of risk of rupture. Morphological and hemodynamic rupture predictors should be validated in studies of prerupture aneurysms.

9.3 Predicting rupture

For morphological and hemodynamic parameters to aid treatment decisions of IA patients, we need knowledge about which factors are associated with rupture, and software applications that allow morphological and hemodynamic analyses to be routinely integrated in the diagnostic workup of daily clinical practice.

9.3.1 Characteristics of prerupture aneurysms

9.3.1.1 Hemodynamic parameters

Paper II suggested that larger areas of low WSS and a concentrated inflow jet might constitute some of the earliest detectable hemodynamic patterns of increased rupture risk.

Low or stagnant flow may trigger an inflammatory response that promotes atherogenesis and leukocyte infiltration.[108] In histological analyses of ruptured and unruptured aneurysms, Frösen et al. found that ruptured aneurysms were characterized by inflammatory infiltration as well as apoptosis and degeneration of the wall matrix.[53]

Our findings are in accordance with other studies indicating that hemodynamic parameters might predict rupture. Takao et al. found significantly lower PLc among 13 internal carotid artery (ICA) and MCA aneurysms that later ruptured, compared with 87 control aneurysms. The 7 ICA aneurysms in the study also had lower minimum WSS.[153] However, the authors did not report patient characteristics, and although the aneurysms belonged to the same size category, the mean size was larger for aneurysms that later ruptured than for those that did not. Duan et al. matched 6 patients with PCoA aneurysms that later ruptured to 4 controls each, based on clinical factors. The aneurysms that later ruptured showed larger LSA and lower normalized WSS. Case and control aneurysms were not matched for size, and the mean size was significantly larger for the aneurysms that later ruptured (mean 7.8 mm) than for those that did not (mean 4.7 mm).[34] Because of the differences between cases and controls in the studies by Takao et al. and Duan et al., level of confounding is unknown.

To our knowledge, Paper II was the first study that matched cases and controls on both patient and aneurysmal characteristics. IA growth and rupture are considered to be closely related, and our finding of an increased LSA among IA that subsequently ruptured is supported by a matched case-control study of IA growth. The study found statistically significantly larger LSA in 12 aneurysms that grew for at least 1 year, compared with 12 stable aneurysms.[16] Still, our findings must be validated in larger studies with a similar matching on or adjusting for patient and aneurysm characteristics.

9.3.1.2 Morphological parameters

In Paper III, the morphology of the included unruptured IAs was largely unable to predict later rupture. An important exception was a straighter Inflow Angle in aneurysms that later ruptured.

In three previous studies where up to six IAs ruptured,[34,102,107] a higher Aspect Ratio was significantly associated with rupture. However, none of these studies were matched on or adjusted for IA size, and might simply have observed the relationship between diameter and geometrical indices. A recent study investigated clinical and morphological parameters at baseline for 142 patients, of which 34 experienced aneurysm rupture during a median follow-up time of 21 years. In the final multivariable regression model, only aneurysm diameter ≥ 7 mm predicted rupture. Morphological indices measured on 2-dimensional angiograms, including Aspect Ratio and Volume-to-ostium Ratio, were only significant when investigated separately from aneurysm diameter and volume.[75] In our study, on the other hand, we were able to perform measurements on 3-dimensional models.

Simulation of hemodynamics provides possible explanations for our finding. In a CFD analysis of idealized geometric models, an inflow angle more aligned with the parent artery exhibited higher jet velocity and kinetic energy as well as higher WSS and WSS gradients.[6,22] In another CFD study of 21 patient-specific models, inflow angles more parallel to the parent artery had a tendency of jet flow pattern and uneven distribution of unsteady pressure, compared to aneurysms with a main axis perpendicular to the parent artery.[22,151] Thus, inflow angles more parallel to the parent artery may result in an unfavorable distribution of hemodynamic forces, leading to quicker aneurysm growth, to points susceptible to perforation by the jet, or to spots with decreased WSS and consecutive weakening.

9.3.1.3 IA development between time of diagnosis and rupture

Irregular appearance of the IA wall represents a higher risk of rupture in other studies,[79,157] but was not statistically significantly associated with rupture in Paper III. Parameters such as irregularity can be viewed as macroscopic manifestations of underlying hemodynamic, cellular and humoral factors.[40] Our findings did *not* show that blebs do not increase rupture risk—the aneurysms may have developed blebs between the time of the angiogram and rupture. Rather, the results showed that, at this early stage, blebs did not serve as a statistically significant rupture predictor in our study.

Our findings suggest that the long-term predictive value of most morphological parameters is limited, perhaps except inflow angle. Still, Papers II and III are snapshots of IA morphology and hemodynamics at a given time in their development. The time of diagnosis of an unruptured IA is clinically important because it is the first time a treatment decision must be made. However, in a

literature review of 30 unruptured IA <7 mm followed with serial imaging for a median of 6.5 years before rupture, 27 (90%) IA enlarged before rupture.[27] A study of aneurysms right before rupture might reveal larger differences between cases and controls than in our studies.

9.3.2 Clinical application of hemodynamics and morphology

The matching on clinical risk factors was paramount for our investigations of aneurysm-related rupture predictors in Papers II and III. But clinical factors affect IA hemodynamics and morphology,[17,64] and hemodynamic and morphological differences between high- and low-risk IA may therefore be larger in the general unmatched population.

Treatment decisions of IA patients must consider both patient- and aneurysm-related risk factors for rupture.[82,155] Knowledge about hemodynamic and morphological parameters is still limited, but may serve as valuable decision support with respect to IA treatment in the future. Clinicians and researchers are already developing tools to integrate these parameters into the evaluation of IA.

There are two important obstacles for the clinical use of hemodynamic and morphological parameters. First, hemodynamic simulation relies on segmentation of angiographies into models, which traditionally has been a time-consuming process. However, Berg et al. recently showed that four physicians were able to segment and simulate models of IA with results comparable to those made by a CFD engineer, though the lowest resolutions underestimated WSS levels. Using a low spatial and temporal resolution, the simulation time for several of the cases was only 10-30 minutes, whereas the usual simulation time is several days.[11] Thus, segmentation and simulation can be feasible in a day-to-day clinical practice.

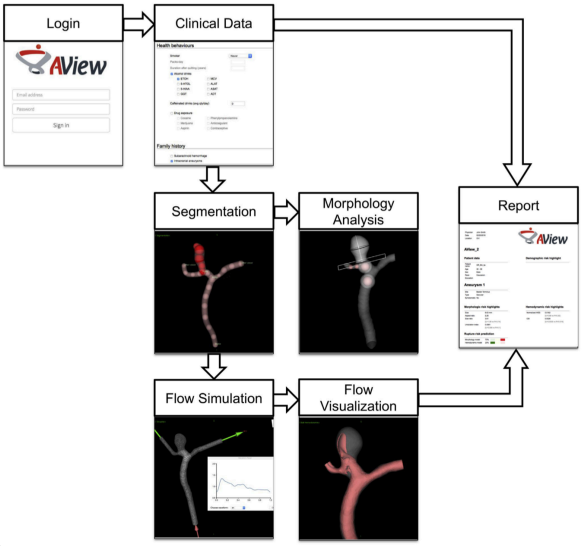

Figure 14. AView workflow consisting of clinical data, segmentation, morphology analysis, flow simulation, and report modules. Reprinted from Xiang J, Varble N, Davies JM, Rai AT, Kono K, Sugiyama S, et al: Initial Clinical Experience with AView—A Clinical Computational Platform for Intracranial Aneurysm Morphology, Hemodynamics, and Treatment Management. ***World Neurosurg 108****:534–542, 2017, with permission from Elsevier.*

Second, prototypes of software applications to facilitate rapid assessment of hemodynamics and morphology in clinical settings have been developed. AView, created by Xiang et al.,[175,176] integrates patient- and aneurysm-related factors and visualizes intraaneurysmal flow. The tool has been distributed to select centers to test technical feasibility, and has

been shown to improve the accuracy of morphological assessment compared to the regular evaluation conducted by neuroradiologists on 2-dimensional images.[128] Figure 14 shows the AView interface and workflow.

Developing prospective registries of IAs can incorporate hemodynamic and morphological parameters. In addition to providing important epidemiological data, such registries can be important sources for further research and validation of these parameters.

9.4 Directions for future research

Because improved treatment of complications of aSAH can have only minor effects on the outcome,[133] improved IA rupture prediction is the most promising way of reducing mortality and morbidity from aSAH. Below, four areas in need of future research are outlined.

First, future studies must expand our knowledge about the prevalence and natural history of IA, since this knowledge is a prerequisite for reliable estimates of rupture risk. In an effort to provide better data on IA prevalence, around 2,000 individuals from the general population will have cerebral imaging using MRI as a part of the Tromsø cohort study, Tromsø, Norway. Similar studies, with subsequent prospective follow-up, are desired for various ethnic groups and locations around the globe.

Second, in light of the results of Paper I, we discourage the use of postrupture IA as a surrogate for prerupture aneurysms in the evaluation of rupture risk—hemodynamic and morphological parameters should be investigated in prerupture aneurysms. The rupture predictors identified in Papers II and III need validation in larger studies. Also, we encourage follow-up imaging to evaluate IA stability and possible morphological and hemodynamic development from diagnosis to growth or rupture, and further research into IA biology and hemodynamics.

Third, we hypothesize that a ratio of IA size and Inflow Angle might be useful in evaluating the risk of IA rupture, because in Paper III, there was a strong correlation between Maximal Size and a straighter Inflow Angle among cases only. Such a ratio would not yield any extra information in our size-matched study, but we encourage fellow researchers to investigate this in unmatched materials.

Fourth, technical advances and research is desired to reduce uncertainty and time consumption of segmentation and simulation procedures. Increased MRI resolution gives information about wall composition and thickness, which can be included in future studies along with patient-specific data on blood pressure and velocity. Intuitive and accessible software applications must provide the clinician with rapid access to the information needed for treatment decisions. The advent of automated

approaches for segmentation and simulation, and 4-dimensional imaging, which incorporates time, open up vast possibilities for integrating aneurysm- and patient-related factors in the evaluation of IA rupture risk.

10 Conclusions

General conclusion

Hemodynamic and morphological parameters of unruptured intracranial aneurysms can be different between those that rupture in the future than in those that remain unruptured. This difference can aid the evaluation of risk of rupture, but the predictive value of each parameter remains uncertain.

Specific conclusions

I. The postrupture morphology of intracranial aneurysms is inadequate as a surrogate for the prerupture morphology.

II. A larger low shear area (LSA) might be an early hemodynamic predictor of intracranial aneurysm rupture.

III. The long-time predictive value of most common morphological parameters may be limited. However, an inflow angle more parallel to the flow direction in the parent artery might be an early morphological predictor of intracranial aneurysm rupture.

11 References

1. Al-Shahi Salman R, Sudlow CL: Case fatality after subarachnoid haemorrhage: declining, but why? **Lancet Neurol 8**:598–599, 2009

2. Alg VS, Sofat R, Houlden H, Werring DJ: Genetic risk factors for intracranial aneurysms: a meta-analysis in more than 116,000 individuals. **Neurology 80**:2154–2165, 2013

3. Backes D, Rinkel GJE, Greving JP, Velthuis BK, Murayama Y, Takao H, et al: ELAPSS score for prediction of risk of growth of unruptured intracranial aneurysms. **Neurology 88**:1600–1606, 2017

4. Backes D, Rinkel GJ, Laban KG, Algra A, Vergouwen MD: Patient- and Aneurysm-Specific Risk Factors for Intracranial Aneurysm Growth: A Systematic Review and Meta-Analysis. **Stroke 47**:951–957, 2016

5. Backes D, Vergouwen MD, Velthuis BK, van der Schaaf IC, Bor AS, Algra A, et al: Difference in aneurysm characteristics between ruptured and unruptured aneurysms in patients with multiple intracranial aneurysms. **Stroke 45**:1299–1303, 2014

6. Baharoglu MI, Schirmer CM, Hoit DA, Gao BL, Malek AM: Aneurysm inflow-angle as a discriminant for rupture in sidewall cerebral aneurysms: morphometric and computational fluid dynamic analysis. **Stroke 41**:1423–1430, 2010

7. Bazilevs Y, Calo VM, Zhang Y, Hughes TJR: Isogeometric Fluid–structure Interaction Analysis with Applications to Arterial Blood Flow. **Comput Mech 38**:310–322, 2006

8. Bazilevs Y, Hsu MC, Zhang Y, Wang W, Kvamsdal T, Hentschel S, et al: Computational vascular fluid-structure interaction: methodology and application to cerebral aneurysms. **Biomech Model Mechanobiol 9**:481–498, 2010

9. Bazilevs Y, Hsu MC, Zhang Y, Wang W, Liang X, Kvamsdal T, et al: A fully-coupled fluid-structure interaction simulation of cerebral aneurysms. **Comput Mech 46**:3–16, 2010

10. Bender MT, Wendt H, Monarch T, Beaty N, Lin L-M, Huang J, et al: Small Aneurysms Account for the Majority and Increasing Percentage of Aneurysmal Subarachnoid Hemorrhage: A 25-Year, Single Institution Study. [E-published ahead of print]. **Neurosurgery**:2017

11. Berg P, Vos S, Becker M, Serowy S, Redel T, Janiga G, et al: Bringing hemodynamic simulations closer to the clinics: a CFD prototype study for intracranial aneurysms. **Conf Proc Annu Int Conf IEEE Eng Med Biol Soc 2016**:3302–3305, 2016

12. Bhopal R: **Concepts of Epidemiology: Integrating the Ideas, Theories, Principles and Methods of Epidemiology**. Oxford: Oxford University Press, 2008

13. Bor ASE, Koffijberg H, Wermer MJH, Rinkel GJE: Optimal screening strategy for familial intracranial aneurysms: A cost-effectiveness analysis. **Neurology 74**:1671–1679, 2010

14. Bor AS, Tiel Groenestege AT, terBrugge KG, Agid R, Velthuis BK, Rinkel GJ, et al: Clinical, radiological, and flow-related risk factors for growth of untreated, unruptured intracranial aneurysms. **Stroke 46**:42–48, 2015

15. Boron W, Boulpaep E: **Medical Physiology**. 2nd Update., Philadelphia, PA: Saunders, 2011

16. Brinjikji W, Chung BJ, Jimenez C, Putman C, Kallmes DF, Cebral JR: Hemodynamic differences between unstable and stable unruptured aneurysms independent of size and location: a pilot study. **J Neurointerv Surg 9**:376–380, 2017

17. Brinjikji W, Zhu YQ, Lanzino G, Cloft HJ, Murad MH, Wang Z, et al: Risk Factors for Growth of Intracranial Aneurysms: A Systematic Review and Meta-Analysis. **AJNR Am J Neuroradiol 37**:615–620, 2016

18. Brisman JL, Song JK, Newell DW, Sonsg JK, Newell DW: Cerebral Aneurysms. **N Engl J Med 355**:928–939, 2006

19. Brown Jr. RD, Broderick JP: Unruptured intracranial aneurysms: epidemiology, natural history, management options, and familial screening. **Lancet Neurol 13**:393–404, 2014

20. Cebral JR, Castro MA, Burgess JE, Pergolizzi RS, Sheridan MJ, Putman CM: Characterization of cerebral aneurysms for assessing risk of rupture by using patient-specific computational hemodynamics models. **AJNR Am J Neuroradiol 26**:2550–2559, 2005

21. Cebral JR, Mut F, Weir J, Putman C: Quantitative characterization of the hemodynamic environment in ruptured and unruptured brain aneurysms. **AJNR Am J Neuroradiol 32**:145–151, 2011

22. Cebral JR, Raschi M: Suggested connections between risk factors of intracranial aneurysms: a review. **Ann Biomed Eng 41**:1366–1383, 2013

23. Chalouhi N, Hoh BL, Hasan D: Review of cerebral aneurysm formation, growth, and rupture. **Stroke 44**:3613–3622, 2013

24. Chalouhi N, Chitale R, Jabbour P, Tjoumakaris S, Dumont AS, Rosenwasser R, et al: The case for family screening for intracranial aneurysms. **Neurosurg Focus 31**:E8, 2011

25. Chatzizisis YS, Coskun AU, Jonas M, Edelman ER, Feldman CL, Stone PH: Role of endothelial shear stress in the natural history of coronary atherosclerosis and vascular remodeling: molecular, cellular, and vascular behavior. **J Am Coll Cardiol 49**:2379–2393, 2007

26. Chien S: Mechanotransduction and endothelial cell homeostasis: the wisdom of the cell. **Am J Physiol Hear Circ Physiol 292**:H1209-24, 2007

27. Chmayssani M, Rebeiz JG, Rebeiz TJ, Batjer HH, Bendok BR: Relationship of growth to aneurysm rupture in asymptomatic aneurysms ≤ 7 mm: A systematic analysis of the literature. **Neurosurgery 68**:1164–1171, 2011

28. Chua MH, Griessenauer CJ, Stapleton CJ, He L, Thomas AJ, Ogilvy CS: Documentation of Improved Outcomes for Intracranial Aneurysm Management Over a 15-Year Interval. **Stroke 47**:708–12, 2016

29. Connolly ES, Rabinstein AA, Carhuapoma JR, Derdeyn CP, Dion J, Higashida RT, et al: Guidelines for the management of aneurysmal subarachnoid hemorrhage: a guideline for healthcare professionals from the American Heart Association/American Stroke Association. **Stroke 43**:1711–37, 2012

30. Costanzo F, Brasseur JG: The invalidity of the Laplace law for biological vessels and of estimating elastic modulus from total stress vs. strain: a new practical method. **Math Med Biol 32**:1–37, 2015

31. de Rooij NK, Linn FH, van der Plas JA, Algra A, Rinkel GJ: Incidence of subarachnoid haemorrhage: a systematic review with emphasis on region, age, gender and time trends. **J Neurol Neurosurg Psychiatry 78**:1365–1372, 2007

32. Dhar S, Tremmel M, Mocco J, Kim M, Yamamoto J, Siddiqui AH, et al: Morphology parameters for intracranial aneurysm rupture risk assessment. **Neurosurgery 63**:185–187, 2008

33. Dorhout Mees S, Rinkel GJ, Feigin VL, Algra A, van den Bergh WM, Vermeulen M, et al: Calcium antagonists for aneurysmal subarachnoid haemorrhage, in Rinkel GJ (ed): **Cochrane Database of Systematic Reviews.** Chichester, UK: John Wiley & Sons, Ltd, 2007, p CD000277

34. Duan G, Lv N, Yin J, Xu J, Hong B, Xu Y, et al: Morphological and hemodynamic analysis of posterior communicating artery aneurysms prone to rupture: a matched case-control study. **J Neurointerv Surg 8**:47–51, 2016

35. E Stehbens BW: Flow in Glass Models of Arterial Bifurcations and Berry Aneurysms at Low Reynolds Numbers. **Q J Exp Physiol 60**:181–192, 1975

36. Engberg AW, Teasdale TW: Epidemiology of non-traumatic brain injury of sudden onset in Denmark 1994-2002. **Ugeskr Laeger 169**:204–8, 2007

37. Etminan N, Brown Jr. RD, Beseoglu K, Juvela S, Raymond J, Morita A, et al: The unruptured intracranial aneurysm treatment score: a multidisciplinary consensus. **Neurology 85**:881–889, 2015

38. Etminan N, Buchholz BA, Dreier R, Bruckner P, Torner JC, Steiger HJ, et al: Cerebral Aneurysms: Formation, Progression, and Developmental Chronology. **Transl Stroke Res 5**:167–173, 2014

39. Etminan N, Dreier R, Buchholz BA, Beseoglu K, Bruckner P, Matzenauer C, et al: Age of collagen in intracranial saccular aneurysms. **Stroke 45**:1757–1763, 2014

40. Etminan N, Rinkel GJ: Unruptured intracranial aneurysms: development, rupture and preventive management. **Nat Rev Neurol 12**:699–713, 2016

41. Evju O, Valen-Sendstad K, Mardal KA: A study of wall shear stress in 12 aneurysms with respect to different viscosity models and flow conditions. **J Biomech 46**:2802–2808, 2013

42. Feigin VL, Rinkel GJ, Lawes CM, Algra A, Bennett DA, van Gijn J, et al: Risk factors for subarachnoid hemorrhage: an updated systematic review of epidemiological studies. **Stroke**

36:2773–2780, 2005

43. Feigin VL, Krishnamurthi R V., Parmar P, Norrving B, Mensah GA, Bennett DA, et al: Update on the Global Burden of Ischemic and Hemorrhagic Stroke in 1990-2013: The GBD 2013 Study. **Neuroepidemiology 45**:161–176, 2015

44. Feigin VL, Lawes CM, Bennett DA, Barker-Collo SL, Parag V: Worldwide stroke incidence and early case fatality reported in 56 population-based studies: a systematic review. **Lancet Neurol 8**:355–369, 2009

45. Feng DD: **Biomedical Information Technology**. Amsterdam: Academic Press, 2008

46. Ferguson GG: Physical factors in the initiation, growth, and rupture of human intracranial saccular aneurysms. **J Neurosurg 37**:666–677, 1972

47. Fisher CM, Kistler JP, Davis JM: Relation of cerebral vasospasm to subarachnoid hemorrhage visualized by computerized tomographic scanning. **Neurosurgery 6**:1–9, 1980

48. Forget Jr. TR, Benitez R, Veznedaroglu E, Sharan A, Mitchell W, Silva M, et al: A review of size and location of ruptured intracranial aneurysms. **Neurosurgery 49**:1322–1326, 2001

49. Francis SE, Tu J, Qian Y, Avolio AP: A combination of genetic, molecular and haemodynamic risk factors contributes to the formation, enlargement and rupture of brain aneurysms. **J Clin Neurosci 20**:912–918, 2013

50. Freemantle N, Marston L, Walters K, Wood J, Reynolds MR, Petersen I: Making inferences on treatment effects from real world data: propensity scores, confounding by indication, and other perils for the unwary in observational research. **BMJ 347**:f6409, 2013

51. Friedman JA, Piepgras DG, Pichelmann MA, Hansen KK, Brown RD, Wiebers DO: Small cerebral aneurysms presenting with symptoms other than rupture. **Neurology 57**:1212–6, 2001

52. Froelich JJ, Neilson S, Peters-Wilke J, Dubey A, Thani N, Erasmus A, et al: Size and Location of Ruptured Intracranial Aneurysms: A 5-Year Clinical Survey. **World Neurosurg 91**:260–265, 2016

53. Frosen J, Piippo A, Paetau A, Kangasniemi M, Niemela M, Hernesniemi J, et al: Remodeling of saccular cerebral artery aneurysm wall is associated with rupture: histological analysis of 24

unruptured and 42 ruptured cases. **Stroke 35**:2287–2293, 2004

54. Frösen J, Tulamo R, Paetau A, Laaksamo E, Korja M, Laakso A, et al: Saccular intracranial aneurysm: pathology and mechanisms. **Acta Neuropathol 123**:773–786, 2012

55. Geers AJ, Larrabide I, Radaelli AG, Bogunovic H, Kim M, Gratama van Andel HAF, et al: Patient-specific computational hemodynamics of intracranial aneurysms from 3D rotational angiography and CT angiography: an in vivo reproducibility study. **AJNR Am J Neuroradiol 32**:581–6, 2011

56. Ghodsi SR, Esfahanian V, Ghodsi SM: Modeling Requirements for Computer Simulation of Cerebral Aneurysm. **J Comput Med 2014**:1–9, 2014

57. Gisev N, Bell JS, Chen TF: Interrater agreement and interrater reliability: key concepts, approaches, and applications. **Res Soc Adm Pharm 9**:330–338, 2013

58. Goubergrits L, Schaller J, Kertzscher U, Petz C, Hege HC, Spuler A: Reproducibility of image-based analysis of cerebral aneurysm geometry and hemodynamics: an in-vitro study of magnetic resonance imaging, computed tomography, and three-dimensional rotational angiography. **J Neurol Surg A Cent Eur Neurosurg 74**:294–302, 2013

59. Greving JP, Wermer MJ, Brown Jr. RD, Morita A, Juvela S, Yonekura M, et al: Development of the PHASES score for prediction of risk of rupture of intracranial aneurysms: a pooled analysis of six prospective cohort studies. **Lancet Neurol 13**:59–66, 2014

60. Guglielmi G, Viñuela F, Sepetka I, Macellari V: Electrothrombosis of saccular aneurysms via endovascular approach. Part 1: Electrochemical basis, technique, and experimental results. **J Neurosurg 75**:1–7, 1991

61. Hackett ML, Anderson CS: Health outcomes 1 year after subarachnoid hemorrhage: An international population-based study. The Australian Cooperative Research on Subarachnoid Hemorrhage Study Group. **Neurology 55**:658–62, 2000

62. Hashimoto T, Meng H, Young WL: Intracranial aneurysms: links among inflammation, hemodynamics and vascular remodeling. **Neurol Res 28**:372–380, 2006

63. Hatze H: Letter: The meaning of the term “biomechanics.” **J Biomech 7**:189–90, 1974

64. Ho AL, Lin N, Frerichs KU, Du R: Smoking and Intracranial Aneurysm Morphology. **Neurosurgery 77**:59–66; discussion 66, 2015

65. Hoi Y, Wasserman BA, Xie YJ, Najjar SS, Ferruci L, Lakatta EG, et al: Characterization of volumetric flow rate waveforms at the carotid bifurcations of older adults. **Physiol Meas 31**:291–302, 2010

66. Hostettler IC, Alg VS, Shahi N, Jichi F, Bonner S, Walsh D, et al: Characteristics of Unruptured Compared to Ruptured Intracranial Aneurysms: A Multicenter Case-Control Study. [E-published ahead of print]. **Neurosurgery**:2017

67. International Study of Unruptured Intracranial Aneurysms Investigators: Unruptured intracranial aneurysms--risk of rupture and risks of surgical intervention. **N Engl J Med 339**:1725–1733, 1998

68. Investigators. UJ, Morita A, Kirino T, Hashi K, Aoki N, Fukuhara S, et al: The natural course of unruptured cerebral aneurysms in a Japanese cohort. **N Engl J Med 366**:2474–2482, 2012

69. Ioannidis JP: Why most published research findings are false. **PLoS Med 2**:e124, 2005

70. Jiménez-Roldán L, Alén JF, Gómez PA, Lobato RD, Ramos A, Munarriz PM, et al: Volumetric analysis of subarachnoid hemorrhage: assessment of the reliability of two computerized methods and their comparison with other radiographic scales. **J Neurosurg 118**:84–93, 2013

71. Johnston SC: Leaving Tiny, Unruptured Intracranial Aneurysms Untreated. **JAMA Neurol 75**:13, 2018

72. Joo SW, Lee SI, Noh SJ, Jeong YG, Kim MS, Jeong YT: What Is the Significance of a Large Number of Ruptured Aneurysms Smaller than 7 mm in Diameter? **J Korean Neurosurg Soc 45**:85–89, 2009

73. Juvela S, Poussa K, Lehto H, Porras M: Natural history of unruptured intracranial aneurysms: a long-term follow-up study. **Stroke 44**:2414–2421, 2013

74. Juvela S: Treatment options of unruptured intracranial aneurysms. **Stroke 35**:372–4, 2004

75. Juvela S, Korja M: Intracranial Aneurysm Parameters for Predicting a Future Subarachnoid

Hemorrhage: A Long-Term Follow-up Study. **Neurosurgery 81**:432–440, 2017

76. Kalanithi P: **When Breath Becomes Air**. New York: Random House, 2016

77. Kallmes DF: Point: CFD--computational fluid dynamics or confounding factor dissemination. **AJNR Am J Neuroradiol 33**:395–396, 2012

78. Kang H, Ji W, Qian Z, Li Y, Jiang C, Wu Z, et al: Aneurysm Characteristics Associated with the Rupture Risk of Intracranial Aneurysms: A Self-Controlled Study. **PLoS One 10**:e0142330, 2015

79. Kleinloog R, de Mul N, Verweij BH, Post JA, Rinkel GJE, Ruigrok YM: Risk Factors for Intracranial Aneurysm Rupture: A Systematic Review. [E-published ahead of print]. **Neurosurgery**:2017

80. Koffijberg H, Buskens E, Algra A, Wermer MJ, Rinkel GJ: Growth rates of intracranial aneurysms: exploring constancy. **J Neurosurg 109**:176–185, 2008

81. Kono K, Tomura N, Yoshimura R, Terada T: Changes in wall shear stress magnitude after aneurysm rupture. **Acta Neurochir 155**:1559–1563, 2013

82. Korja M, Kaprio J: Controversies in epidemiology of intracranial aneurysms and SAH. **Nat Rev Neurol 12**:50–55, 2016

83. Korja M, Lehto H, Juvela S: Lifelong rupture risk of intracranial aneurysms depends on risk factors: a prospective Finnish cohort study. **Stroke 45**:1958–1963, 2014

84. Korja M, Silventoinen K, McCarron P, Zdravkovic S, Skytthe A, Haapanen A, et al: Genetic epidemiology of spontaneous subarachnoid hemorrhage: Nordic Twin Study. **Stroke 41**:2458–2462, 2010

85. Korja M, Lehto H, Juvela S, Kaprio J: Incidence of subarachnoid hemorrhage is decreasing together with decreasing smoking rates. **Neurology 87**:1118–1123, 2016

86. Korja M, Silventoinen K, Laatikainen T, Jousilahti P, Salomaa V, Hernesniemi J, et al: Risk factors and their combined effects on the incidence rate of subarachnoid hemorrhage--a population-based cohort study. **PLoS One 8**:e73760, 2013

87. Korja M, Silventoinen K, Laatikainen T, Jousilahti P, Salomaa V, Kaprio J: Cause-specific mortality of 1-year survivors of subarachnoid hemorrhage. **Neurology 80**:481–6, 2013

88. Kotowski M, Naggara O, Darsaut TE, Nolet S, Gevry G, Kouznetsov E, et al: Safety and occlusion rates of surgical treatment of unruptured intracranial aneurysms: a systematic review and meta-analysis of the literature from 1990 to 2011. **J Neurol Neurosurg Psychiatry 84**:42–48, 2013

89. Lasheras JC: The Biomechanics of Arterial Aneurysms. **Annu Rev Fluid Mech 39**:293–319, 2007

90. Lauric A, Baharoglu MI, Malek AM: Ruptured status discrimination performance of aspect ratio, height/width, and bottleneck factor is highly dependent on aneurysm sizing methodology. **Neurosurgery 71**:38–45, 2012

91. Lauric A, Hippelheuser J, Cohen AD, Kadasi LM, Malek AM: Wall shear stress association with rupture status in volume matched sidewall aneurysms. **J Neurointerv Surg 6**:466–473, 2014

92. Lauric A, Miller EL, Baharoglu MI, Malek AM: 3D shape analysis of intracranial aneurysms using the writhe number as a discriminant for rupture. **Ann Biomed Eng 39**:1457–1469, 2011

93. Lawton MT, Vates GE: Subarachnoid Hemorrhage. **N Engl J Med 377**:257–266, 2017

94. Li YS, Haga JH, Chien S: Molecular basis of the effects of shear stress on vascular endothelial cells. **J Biomech 38**:1949–1971, 2005

95. Lindekleiv HM, Njolstad I, Ingebrigtsen T, Mathiesen EB: Incidence of aneurysmal subarachnoid hemorrhage in Norway, 1999-2007. **Acta Neurol Scand 123**:34–40, 2011

96. Lindekleiv HM, Valen-Sendstad K, Morgan MK, Mardal KA, Faulder K, Magnus JH, et al: Sex differences in intracranial arterial bifurcations. **Gend Med 7**:149–155, 2010

97. Lindekleiv H, Sandvei MS, Njolstad I, Lochen ML, Romundstad PR, Vatten L, et al: Sex differences in risk factors for aneurysmal subarachnoid hemorrhage: a cohort study. **Neurology 76**:637–643, 2011

98. Lindekleiv H, Sandvei MS, Romundstad PR, Wilsgaard T, Njolstad I, Ingebrigtsen T, et al:

Joint effect of modifiable risk factors on the risk of aneurysmal subarachnoid hemorrhage: a cohort study. **Stroke 43**:1885–1889, 2012

99. Lindekleiv H, Mathiesen EB, Førde OH, Wilsgaard T, Ingebrigtsen T: Hospital volume and 1-year mortality after treatment of intracranial aneurysms: a study based on patient registries in Scandinavia. **J Neurosurg 123**:631–637, 2015

100. Linn FH, Rinkel GJ, Algra A, van Gijn J: Incidence of subarachnoid hemorrhage: role of region, year, and rate of computed tomography: a meta-analysis. **Stroke 27**:625–9, 1996

101. Linn FH, Rinkel GJ, Algra A, van Gijn J: The notion of "warning leaks" in subarachnoid haemorrhage: are such patients in fact admitted with a rebleed? **J Neurol Neurosurg Psychiatry 68**:332–6, 2000

102. Liu J, Fan J, Xiang J, Zhang Y, Yang X: Hemodynamic characteristics of large unruptured internal carotid artery aneurysms prior to rupture: a case control study. **J Neurointerv Surg 8**:367–372, 2016

103. Logg A, Mardal K-A, Wells GN, eds., Logg A, Mardal K-A, et al: **Automated Solution of Differential Equations by the Finite Element Method**. Heidelberg: Springer, 2012

104. Lucke-Wold BP, Logsdon AF, Manoranjan B, Turner RC, McConnell E, Vates GE, et al: Aneurysmal Subarachnoid Hemorrhage and Neuroinflammation: A Comprehensive Review. **Int J Mol Sci 17**:2016

105. Malhotra A, Wu X, Forman HP, Matouk CC, Gandhi D, Sanelli P: Management of Tiny Unruptured Intracranial Aneurysms. **JAMA Neurol 75**:27, 2018

106. Matsuda M, Watanabe K, Saito A, Matsumura K, Ichikawa M: Circumstances, Activities, and Events Precipitating Aneurysmal Subarachnoid Hemorrhage. **J Stroke Cerebrovasc Dis 16**:25–29, 2007

107. Mehan Jr. WA, Romero JM, Hirsch JA, Sabbag DJ, Gonzalez RG, Heit JJ, et al: Unruptured intracranial aneurysms conservatively followed with serial CT angiography: could morphology and growth predict rupture? **J Neurointerv Surg 6**:761–766, 2014

108. Meng H, Tutino VM, Xiang J, Siddiqui A: High WSS or Low WSS? Complex Interactions of Hemodynamics with Intracranial Aneurysm Initiation, Growth, and Rupture: Toward a

Unifying Hypothesis. **AJNR Am J Neuroradiol 35**:1254–1262, 2014

109. Molyneux AJ, Birks J, Clarke A, Sneade M, Kerr RSC: The durability of endovascular coiling versus neurosurgical clipping of ruptured cerebral aneurysms: 18 year follow-up of the UK cohort of the International Subarachnoid Aneurysm Trial (ISAT). **Lancet 385**:691–697, 2015

110. Molyneux AJ, Kerr RS, Yu LM, Clarke M, Sneade M, Yarnold JA, et al: International subarachnoid aneurysm trial (ISAT) of neurosurgical clipping versus endovascular coiling in 2143 patients with ruptured intracranial aneurysms: a randomised comparison of effects on survival, dependency, seizures, rebleeding, subgroups, and . **Lancet 366**:809–817, 2005

111. Molyneux A, Kerr R, Stratton I, Sandercock P, Clarke M, Shrimpton J, et al: International Subarachnoid Aneurysm Trial (ISAT) of neurosurgical clipping versus endovascular coiling in 2143 patients with ruptured intracranial aneurysms: a randomised trial. **Lancet 360**:1267–1274, 2002

112. Morris PD, Narracott A, von Tengg-Kobligk H, Silva Soto DA, Hsiao S, Lungu A, et al: Computational fluid dynamics modelling in cardiovascular medicine. **Heart 102**:18–28, 2016

113. Muller TB, Sandvei MS, Kvistad KA, Rydland J, Haberg A, Vik A, et al: Unruptured intracranial aneurysms in the Norwegian Nord-Trondelag Health Study (HUNT): risk of rupture calculated from data in a population-based cohort study. **Neurosurgery 73**:256–61; discussion 260; quiz 261, 2013

114. Naggara ON, Lecler A, Oppenheim C, Meder J-F, Raymond J: Endovascular Treatment of Intracranial Unruptured Aneurysms: A Systematic Review of the Literature on Safety with Emphasis on Subgroup Analyses. **Radiology 263**:828–835, 2012

115. Naggara ON, White PM, Guilbert F, Roy D, Weill A, Raymond J: Endovascular Treatment of Intracranial Unruptured Aneurysms: Systematic Review and Meta-Analysis of the Literature on Safety and Efficacy. **Radiology 256**:887–97, 2010

116. Niemczyk M, Gradzik M, Niemczyk S, Bujko M, Golebiowski M, Paczek L: Intracranial aneurysms in autosomal dominant polycystic kidney disease. **AJNR Am J Neuroradiol 34**:1556–1559, 2013

117. Nieuwkamp DJ, Setz LE, Algra A, Linn FH, de Rooij NK, Rinkel GJ: Changes in case fatality

of aneurysmal subarachnoid haemorrhage over time, according to age, sex, and region: a meta-analysis. **Lancet Neurol 8**:635–642, 2009

118. Niven DJ, Berthiaume LR, Fick GH, Laupland KB: Matched case-control studies: a review of reported statistical methodology. **Clin Epidemiol 4**:99–110, 2012

119. OCEBM Levels of Evidence Working Group: The Oxford Levels of Evidence 2. **Oxford Cent Evidence-Based Med** Available: http://www.cebm.net/index.aspx?o=5653. Accessed 8 December 2017

120. Ohkuma H, Tsurutani H, Suzuki S: Incidence and significance of early aneurysmal rebleeding before neurosurgical or neurological management. **Stroke 32**:1176–80, 2001

121. Orbo M, Waterloo K, Egge A, Isaksen J, Ingebrigtsen T, Romner B: Predictors for cognitive impairment one year after surgery for aneurysmal subarachnoid hemorrhage. **J Neurol 255**:1770–1776, 2008

122. Patel RL, Richards P, Chambers DJ, Venn G: Infective endocarditis complicated by ruptured cerebral mycotic aneurysm. **J R Soc Med 84**:746–7, 1991

123. Piccinelli M, Steinman DA, Hoi Y, Tong F, Veneziani A, Antiga L: Automatic neck plane detection and 3D geometric characterization of aneurysmal sacs. **Ann Biomed Eng 40**:2188–2211, 2012

124. Pierot L, Wakhloo AK: Endovascular treatment of intracranial aneurysms: current status. **Stroke 44**:2046–54, 2013

125. Polmear A: Sentinel Headaches in Aneurysmal Subarachnoid Haemorrhage: What is the True Incidence? A Systematic Review. **Cephalalgia 23**:935–941, 2003

126. Raghavan ML, Kratzberg JA, Golzarian J: Introduction to biomechanics related to endovascular repair of abdominal aortic aneurysm. **Tech Vasc Interv Radiol 8**:50–55, 2005

127. Rahman M, Ogilvy CS, Zipfel GJ, Derdeyn CP, Siddiqui AH, Bulsara KR, et al: Unruptured cerebral aneurysms do not shrink when they rupture: multicenter collaborative aneurysm study group. **Neurosurgery 68**:151–155, 2011

128. Rajabzadeh-Oghaz H, Varble N, Davies JM, Mowla A, Shakir HJ, Sonig A, et al: Computer-

Assisted Adjuncts for Aneurysmal Morphologic Assessment: Toward More Precise and Accurate Approaches. **Proc SPIE--the Int Soc Opt Eng 97**:5421–5433, 2017

129. Raps EC, Rogers JD, Galetta SL, Solomon RA, Lennihan L, Klebanoff LM, et al: The clinical spectrum of unruptured intracranial aneurysms. **Arch Neurol 50**:265–8, 1993

130. Ravindra VM, de Havenon A, Gooldy TC, Scoville J, Guan J, Couldwell WT, et al: Validation of the unruptured intracranial aneurysm treatment score: comparison with real-world cerebrovascular practice. [E-published ahead of print]. **J Neurosurg**:2017

131. Rinaldo L, McCutcheon BA, Murphy ME, Shepherd DL, Maloney PR, Kerezoudis P, et al: Quantitative analysis of the effect of institutional case volume on complications after surgical clipping of unruptured aneurysms. [E-published ahead of print]. **J Neurosurg**:2017

132. Rivero-Arias O, Gray A, Wolstenholme J: Burden of disease and costs of aneurysmal subarachnoid haemorrhage (aSAH) in the United Kingdom. **Cost Eff Resour Alloc 8**:6, 2010

133. Roos YB, de Haan RJ, Beenen LF, Groen RJ, Albrecht KW, Vermeulen M: Complications and outcome in patients with aneurysmal subarachnoid haemorrhage: a prospective hospital based cohort study in the Netherlands. **J Neurol Neurosurg Psychiatry 68**:337–41, 2000

134. Rossetti S, Harris PC: The genetics of vascular complications in autosomal dominant polycystic kidney disease (ADPKD). **Curr Hypertens Rev 9**:37–43, 2013

135. Sandvei MS, Lindekleiv H, Romundstad PR, Muller TB, Vatten LJ, Ingebrigtsen T, et al: Risk factors for aneurysmal subarachnoid hemorrhage - BMI and serum lipids: 11-year follow-up of the HUNT and the Tromso Study in Norway. **Acta Neurol Scand 125**:382–388, 2012

136. Sandvei MS, Mathiesen EB, Vatten LJ, Muller TB, Lindekleiv H, Ingebrigtsen T, et al: Incidence and mortality of aneurysmal subarachnoid hemorrhage in two Norwegian cohorts, 1984-2007. **Neurology 77**:1833–1839, 2011

137. Sato K, Yoshimoto Y: Risk profile of intracranial aneurysms: rupture rate is not constant after formation. **Stroke 42**:3376–3381, 2011

138. Schneiders JJ, Marquering HA, van den Berg R, VanBavel E, Velthuis B, Rinkel GJ, et al: Rupture-associated changes of cerebral aneurysm geometry: high-resolution 3D imaging before and after rupture. **AJNR Am J Neuroradiol 35**:1358–1362, 2014

139. Sedgwick P: Multiple hypothesis testing and Bonferroni's correction. **BMJ 349**:g6284, 2014

140. Serrone JC, Tackla RD, Gozal YM, Hanseman DJ, Gogela SL, Vuong SM, et al: Aneurysm growth and de novo aneurysms during aneurysm surveillance. **J Neurosurg 125**:1374–1382, 2016

141. Shojima M, Oshima M, Takagi K, Torii R, Hayakawa M, Katada K, et al: Magnitude and Role of Wall Shear Stress on Cerebral Aneurysm: Computational Fluid Dynamic Study of 20 Middle Cerebral Artery Aneurysms. **Stroke 35**:2500–2505, 2004

142. Shrout PE: Measurement reliability and agreement in psychiatry. **Stat Methods Med Res 7**:301–317, 1998

143. Siddiq F, Biller J, Wilterdink JL: Nonaneurysmal subarachnoid hemorrhage - UpToDate. Available: https://www.uptodate.com/contents/nonaneurysmal-subarachnoid-hemorrhage?source=see_link. Accessed 24 October 2017

144. Skelly AC, Dettori JR, Brodt ED: Assessing bias: the importance of considering confounding. **Evid Based Spine Care J 3**:9–12, 2012

145. Spetzler RF, McDougall CG, Zabramski JM, Albuquerque FC, Hills NK, Russin JJ, et al: The Barrow Ruptured Aneurysm Trial: 6-year results. **J Neurosurg 123**:609–617, 2015

146. Spetzler RF, McDougall CG, Albuquerque FC, Zabramski JM, Hills NK, Partovi S, et al: The Barrow Ruptured Aneurysm Trial: 3-year results. **J Neurosurg 119**:146–157, 2013

147. Steiner T, Juvela S, Unterberg A, Jung C, Forsting M, Rinkel G, et al: European Stroke Organization guidelines for the management of intracranial aneurysms and subarachnoid haemorrhage. **Cerebrovasc Dis 35**:93–112, 2013

148. Steinman DA: Assumptions in modelling of large artery hemodynamics, in Ambrosi D , Quarteroni A , Rozza G (eds): **Modeling of Physiological Flows.** Milano: Springer Milan, 2012, pp 1–18

149. Suarez JI, Tarr RW, Selman WR: Aneurysmal subarachnoid hemorrhage. **N Engl J Med 354**:387–396, 2006

150. Suh SH, Cloft HJ, Huston 3rd J, Han KH, Kallmes DF: Interobserver variability of aneurysm

morphology: discrimination of the daughter sac. **J Neurointerv Surg 8**:38–41, 2016

151. Szikora I, Paal G, Ugron A, Nasztanovics F, Marosfoi M, Berentei Z, et al: Impact of aneurysmal geometry on intraaneurysmal flow: a computerized flow simulation study. **Neuroradiology 50**:411–421, 2008

152. Szklo M, Nieto FJ: **Epidemiology: Beyond the Basics**. Jones & Bartlett Learning, 2014

153. Takao H, Murayama Y, Otsuka S, Qian Y, Mohamed A, Masuda S, et al: Hemodynamic differences between unruptured and ruptured intracranial aneurysms during observation. **Stroke 43**:1436–1439, 2012

154. Teo M, St George EJ: Radiologic Surveillance of Untreated Unruptured Intracranial Aneurysms: A Single Surgeon's Experience. **World Neurosurg 90**:20–28, 2016

155. Thompson BG, Brown Jr. RD, Amin-Hanjani S, Broderick JP, Cockroft KM, Connolly Jr. ES, et al: Guidelines for the Management of Patients With Unruptured Intracranial Aneurysms: A Guideline for Healthcare Professionals From the American Heart Association/American Stroke Association. **Stroke 46**:2368–2400, 2015

156. Torii R, Oshima M, Kobayashi T, Takagi K, Tezduyar TE: Computer modeling of cardiovascular fluid–structure interactions with the deforming-spatial-domain/stabilized space–time formulation. **Comput Methods Appl Mech Eng 195**:1885–1895, 2006

157. Tsukahara T, Murakami N, Sakurai Y, Yonekura M, Takahashi T, Inoue T, et al: Treatment of unruptured cerebral aneurysms; a multi-center study at Japanese national hospitals. **Acta Neurochir Suppl 94**:77–85, 2005

158. Uzan M, Cantasdemir M, Seckin MS, Hanci M, Kocer N, Sarioglu AC, et al: Traumatic intracranial carotid tree aneurysms. **Neurosurgery 43**:1314-20–2, 1998

159. Valen-Sendstad K, Mardal KA, Steinman DA: High-resolution CFD detects high-frequency velocity fluctuations in bifurcation, but not sidewall, aneurysms. **J Biomech 46**:402–407, 2013

160. Valen-Sendstad K, Piccinelli M, KrishnankuttyRema R, Steinman DA: Estimation of inlet flow rates for image-based aneurysm CFD models: where and how to begin? **Ann Biomed Eng 43**:1422–1431, 2015

161. Valen-Sendstad K, Piccinelli M, Steinman DA: High-resolution computational fluid dynamics detects flow instabilities in the carotid siphon: Implications for aneurysm initiation and rupture? **J Biomech**:2014

162. Valen-Sendstad K, Steinman DA: Mind the gap: impact of computational fluid dynamics solution strategy on prediction of intracranial aneurysm hemodynamics and rupture status indicators. **AJNR Am J Neuroradiol 35**:536–543, 2014

163. van Gelder JM: Computed tomographic angiography for detecting cerebral aneurysms: implications of aneurysm size distribution for the sensitivity, specificity, and likelihood ratios. **Neurosurgery 53**:597-605–6, 2003

164. van Gijn J, Rinkel GJ: Subarachnoid haemorrhage: diagnosis, causes and management. **Brain 124**:249–278, 2001

165. Vergouwen MDI, de Haan RJ, Vermeulen M, Roos YBWEM: Effect of Statin Treatment on Vasospasm, Delayed Cerebral Ischemia, and Functional Outcome in Patients With Aneurysmal Subarachnoid Hemorrhage: A Systematic Review and Meta-Analysis Update. **Stroke 41**:e47–e52, 2010

166. Vergouwen MDI, Ilodigwe D, Macdonald RL: Cerebral infarction after subarachnoid hemorrhage contributes to poor outcome by vasospasm-dependent and -independent effects. **Stroke 42**:924–9, 2011

167. Versteeg H, Malalasekera W: **An Introduction to Computational Fluid Dynamics: The Finite Volume Method**. ed 2nd, Harlow: Pearson/Prentice Hall, 2007

168. Villablanca JP, Duckwiler GR, Jahan R, Tateshima S, Martin NA, Frazee J, et al: Natural history of asymptomatic unruptured cerebral aneurysms evaluated at CT angiography: growth and rupture incidence and correlation with epidemiologic risk factors. **Radiology 269**:258–265, 2013

169. Vlak MH, Rinkel GJ, Greebe P, van der Bom JG, Algra A: Trigger factors and their attributable risk for rupture of intracranial aneurysms: a case-crossover study. **Stroke 42**:1878–1882, 2011

170. Vlak MH, Algra A, Brandenburg R, Rinkel GJ: Prevalence of unruptured intracranial

aneurysms, with emphasis on sex, age, comorbidity, country, and time period: a systematic review and meta-analysis. **Lancet Neurol 10**:626–636, 2011

171. von Elm E, Altman DG, Egger M, Pocock SJ, Gotzsche PC, Vandenbroucke JP, et al: The Strengthening the Reporting of Observational Studies in Epidemiology (STROBE) statement: guidelines for reporting observational studies. **Ann Intern Med 147**:573–577, 2007

172. Wermer MJ, van der Schaaf IC, Velthuis BK, Algra A, Buskens E, Rinkel GJ: Follow-up screening after subarachnoid haemorrhage: frequency and determinants of new aneurysms and enlargement of existing aneurysms. **Brain 128**:2421–2429, 2005

173. Wiebers DO, Whisnant JP, Huston 3rd J, Meissner I, Brown Jr. RD, Piepgras DG, et al: Unruptured intracranial aneurysms: natural history, clinical outcome, and risks of surgical and endovascular treatment. **Lancet 362**:103–110, 2003

174. Xiang J, Natarajan SK, Tremmel M, Ma D, Mocco J, Hopkins LN, et al: Hemodynamic-morphologic discriminants for intracranial aneurysm rupture. **Stroke 42**:144–152, 2011

175. Xiang J, Varble N, Davies JM, Rai AT, Kono K, Sugiyama S, et al: Initial Clinical Experience with AView—A Clinical Computational Platform for Intracranial Aneurysm Morphology, Hemodynamics, and Treatment Management. **World Neurosurg 108**:534–542, 2017

176. Xiang J, Antiga L, Varble N, Snyder K V., Levy EI, Siddiqui AH, et al: AView: An Image-based Clinical Computational Tool for Intracranial Aneurysm Flow Visualization and Clinical Management. **Ann Biomed Eng 44**:1085–1096, 2016

177. Yi J, Zielinski D, Chen M: Cerebral Aneurysm Size before and after Rupture: Case Series and Literature Review. **J Stroke Cerebrovasc Dis 25**:1244–1248, 2016

178. Zanaty M, Chalouhi N, Tjoumakaris SI, Fernando Gonzalez L, Rosenwasser RH, Jabbour PM: Aneurysm geometry in predicting the risk of rupture. A review of the literature. **Neurol Res 36**:308–313, 2014

179. Zanaty M, Chalouhi N, Starke RM, Tjoumakaris S, Gonzalez LF, Hasan D, et al: Endovascular treatment of cerebral mycotic aneurysm: a review of the literature and single center experience. **Biomed Res Int 2013**:151643, 2013

180. Zhu R-L, Chen Z-J, Li S, Lu X-C, Tang L-J, Huang B-S, et al: Statin-treated patients with

aneurysmal subarachnoid haemorrhage: a meta-analysis. **Eur Rev Med Pharmacol Sci 20**:2090–8, 2016

181. Zylkowski J, Kunert P, Jaworski M, Rosiak G, Marchel A, Rowinski O: Changes of size and shape of small, unruptured intracranial aneurysms in repeated computed tomography angiography studies. **Wideochir Inne Tech Maloinwazyjne 10**:178–188, 2015

12 Papers

Paper I

Paper II

Paper III